Mullard

Technical Communications

Volume 14 Number 133 January 1977

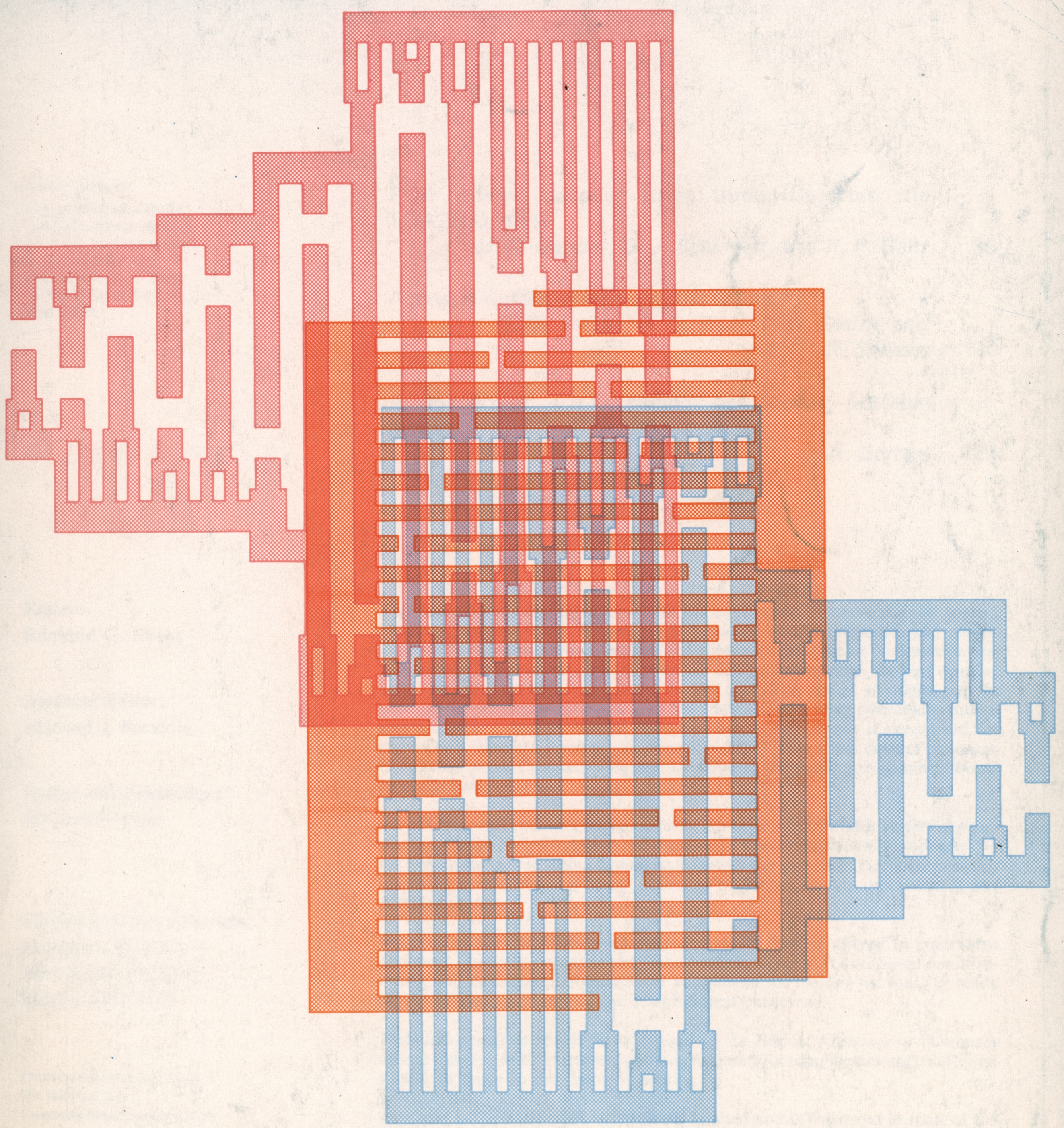

- RGB colour decoder using three ICs from the TDA2500 range
- Acoustic surface-wave bandpass filters
- A low-power v.h.f. paging or pocket portable receiver

Mullard Technical Communications
ISSN 0027—3139

Volume 14 Number 133 January 1977

Cover picture:
Interdigital electrode configurations used in acoustic surface-wave filters; design and manufacture of these filters is described in this issue.

RGB colour decoder using three ICs from the TDA2500 range
M. C. Gander, D. J. Beakhust, and R. P. Gant 86

Acoustic surface-wave bandpass filters
D. W. Parker, R. G. Pratt, F. W. Smith, and R. Stevens 110

A low-power v.h.f. paging or pocket portable receiver
J. A. Garters 125

Editor:
Edmund G. Evans

Assistant Editor:
Michael J. Prescott

Design and Production:
Michael J. Rose

Central Technical Services,
Mullard Limited,
New Road, Mitcham,
Surrey, CR4 4XY

This journal records developments in the application of electronics in science, industry, and the home. It contains information on the properties and performance of solid-state devices, valves and tubes, and associated components and assemblies. The practical circuits given are designed to provide the best working conditions and performance for the devices used. The design principles may be used (so far as device ratings allow) for adaptation to meet particular requirements. Current data should be consulted before any circuit is considered for production. Mullard Limited can normally supply only those devices or assemblies listed in the Company's current catalogues. Availability in quantity should be confirmed.

All information is published in good faith, but because of the wide variety of situations in which this information may be used, we cannot accept any responsibility for loss or damage resulting from unsatisfactory performance. Publication of this information does not imply any authority or licence for the utilisation of any patented feature.

Four issues are published each year and issued free of charge to equipment designers, research organisations, laboratories, libraries, educational establishments, and consultants. Requests for addition to the mailing list must be made on the official stationery of the establishment concerned.

Technical enquiries should be addressed to the Editor. Abstracts or references should mention both source and authors. Requests for republication or translation should be made to the Editor in writing.

'Mullard' is the trade mark of Mullard Limited and is registered in most of the principal countries of the world.

Made and Printed in England by
The Yale Press Ltd.,
Carmichael Road, London, S.E.25.
© Mullard Limited 1977

Mullard Limited, Mullard House, Torrington Place, London WC1E 7HD Tel: 01-580 6633 Telex: 264341

RGB colour decoder using three ICs from the TDA2500 range

M.C. GANDER, D.J. BEAKHUST, and R.P. GANT
Mullard Central Application Laboratory

An economical RGB decoder using three ICs from the TDA2500 range is described. Typical video output stages for use with the decoder are also described, together with two methods of voltage regulation, the alignment procedure, and some optional circuits.

INTRODUCTION

The RGB decoder described in this article uses the TDA2560, TDA2522, and TDA2530 sixteen-lead integrated circuits, and the miniature delay line type DL60. This decoder (Fig.1) offers several advantages over the earlier design described in Ref.1, including a significant reduction in peripheral components, a reduction in the effects of the tolerances of these components on the decoder performance, and simplified alignment. The advantages of the 78M12CU voltage regulator integrated circuit over a simple voltage-regulating network for the h.t. supply of the decoder are described. The decoder is compatible with most types of video output stage, and typical circuits for class A, class AB, and class B stages are also described.

The general environmental conditions for the integrated circuits, including the requirements for power supplies, protection from power supply surges and picture tube flashover energy, and heat considerations are described in Ref.1.

The principal features of the new RGB decoder system are summarised below.

- The black-level stability with contrast control variation and temperature variation is improved. Additional improvements include a low spread in luminance channel gain and reduced sensitivity to ripple in the l.t. supply.
- The black-level clamp is unaffected by white noise on the video signal.
- Linear low-spread electronic controls are provided for luminance and chroma signals. The controls have accurate tracking and permit complete turn-off of chroma. They are suitable for use with local and remote control systems.
- An 8.8MHz subcarrier regenerator eliminates the 90° phase adjustment.
- The use of a common channel for the chroma and burst signals at the input of the PAL delay line results in a reduction in the phase differential between these signals, and therefore eliminates the need for adjustment of burst-phase.
- The spread in insertion loss of the PAL delay line (normally ±3dB) is compensated for by the a.c.c. system.
- Synchronous detection of a.c.c. together with a sample-and-hold technique gives good noise immunity.
- Colour-killer hysteresis is built in to reduce colour flashing on marginal signals.
- A.C. feedback and gated clamping is used over the video output stages, ensuring uniform a.c. response and drift-free d.c. response with excellent rejection of ripple in the h.t. supply.
- Electronic RGB drive controls eliminate any frequency response variation with adjustment of the picture tube drive on the white-point setting.
- An inverted video signal is available for driving a sync separator which requires positive-going sync.

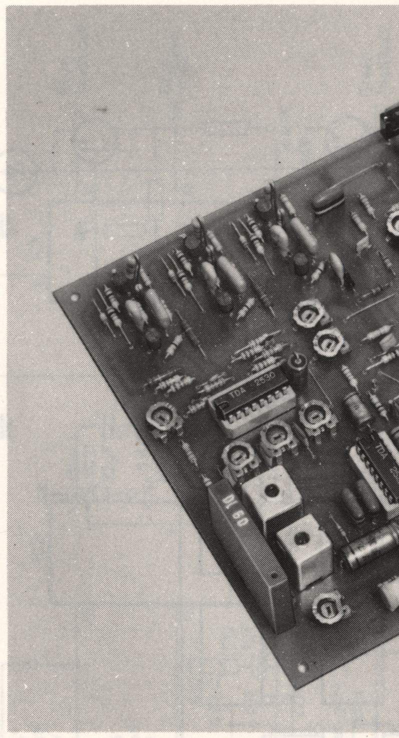

Fig.1 – Photograph showing compact layout of the RGB decoder. Class AB output stages and a voltage regulator IC are included on the board, together with four optional circuits

SYSTEM DESCRIPTION

A block diagram of the decoder system, including some of the principal peripheral components of the three integrated circuits, is shown in Fig.2.

The TDA2560 integrated circuit IC_1 contains the control stages for the luminance and chrominance signals, and for the associated functions of black-level clamping and blanking. Integrated circuit IC_1 also contains the a.c.c.-controlled amplifier and a drive circuit for the PAL delay line type DL60. A balanced chroma signal derived from a chroma bandpass filter operating in push-pull is applied to pins 1 and 2, and the luminance signal is applied to pin 14. The saturation, brightness, and contrast control networks are connected directly to IC_1. The chroma output signal at pin 6 is fed to the PAL delay line through an isolating capacitor, and the output signal from the delay line is combined with the undelayed chroma signal to recover the B–Y and R–Y signals before they are applied to IC_2 (TDA2522).

The luminance signal at pin 10 is obtained from the low-impedance output of an emitter-follower stage, and is applied to the RGB matrix in IC_3 (TDA2530, pin 1).

The TDA2522 integrated circuit IC_2 contains an 8.8MHz reference oscillator (exact frequency 8.867238 MHz), the a.c.c. detector and amplifier, and the synchronous demodulators, together with internal filtering for the colour difference signal outputs. Capacitive coupling is used between the B–Y, G–Y, and R–Y outputs of IC_2 and the inputs of IC_3.

The TDA2530 integrated circuit IC_3 contains the RGB matrix with the provision for d.c. adjustment of the gain of each channel. A.C. signal feedback and gated d.c. feedback are provided over the RGB output stages. The RGB drive signals at pins 10, 12, and 14 are intended for the base-drive of the transistors in simple class A video output stages, and several types of push-pull class AB or B stages.

DECODER CIRCUIT DESCRIPTION

The general circuit of the decoder including the recommended peripheral components for the integrated circuits is shown in Fig.3. This circuit embodies all of the necessary functions of the decoder with the minimum number of components. The decoder in the form shown may be supplied directly with a composite video signal provided by an i.f. amplifier using a TCA270 or TDA2540 integrated circuit. Because the integrated circuits types TDA2560, TDA2522, and TDA2530 have been designed to allow some flexibility in the design of the circuit in which they are used, some variations in parts of the practical circuit of the decoder are possible. These variations will depend on the requirements of the individual user, and some optional circuits for use with the RGB decoder shown in Fig.3 are described at the end of this article. The functions of the peripheral circuits of the three ICs are described below.

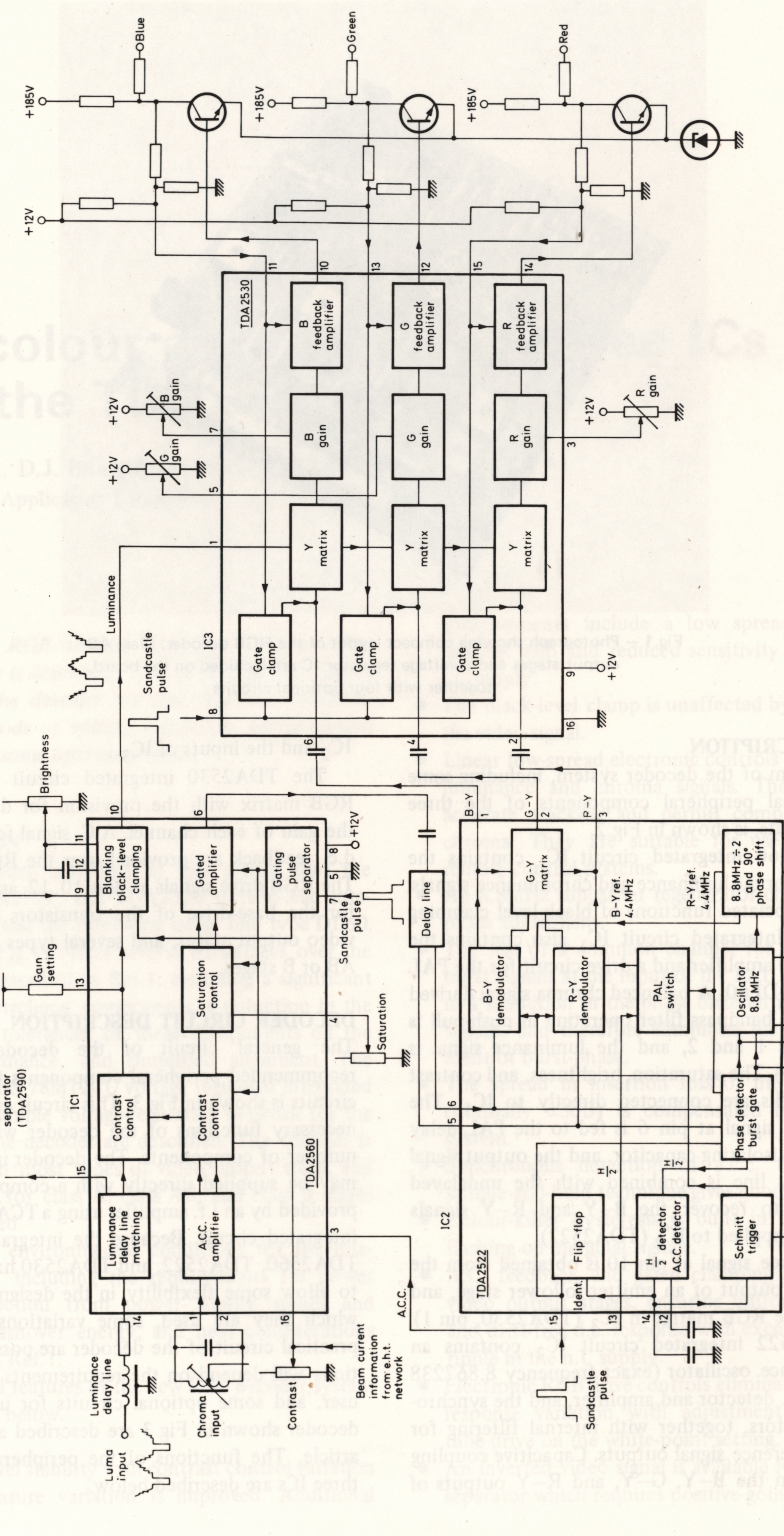
Blue
Green
Red
+185V
+12V
TDA2530
B feedback amplifier
G feedback amplifier
R feedback amplifier
B gain
G gain
R gain
Y matrix
Gate clamp
IC3
Luminance
Sandcastle pulse
Brightness
Blanking black-level clamping
Gated amplifier
Gating pulse separator
Frame and line blanking
Gain setting
Saturation control
Saturation
Contrast control
Luminance output to sync separator (TDA2590)
IC1
TDA2560
Luminance delay line matching
A.C.C. amplifier
Luminance delay line
Luma input
Chroma input
Contrast
Beam current information from e.h.t. network
A.C.C.
Delay line
B-Y
G-Y
R-Y
G-Y matrix
8.8MHz ÷2 and 90° phase shift
B-Yref 4.4MHz
R-Yref 4.4MHz
B-Y demodulator
R-Y demodulator
PAL switch
Oscillator 8.8MHz
Phase detector burst gate
H/2
Ident.
Flip-flop
H/2 detector ACC detector
Schmitt trigger
Colour killer delay
IC2
TDA2522
Sandcastle pulse
8572

Fig.2 – Block diagram of decoder system

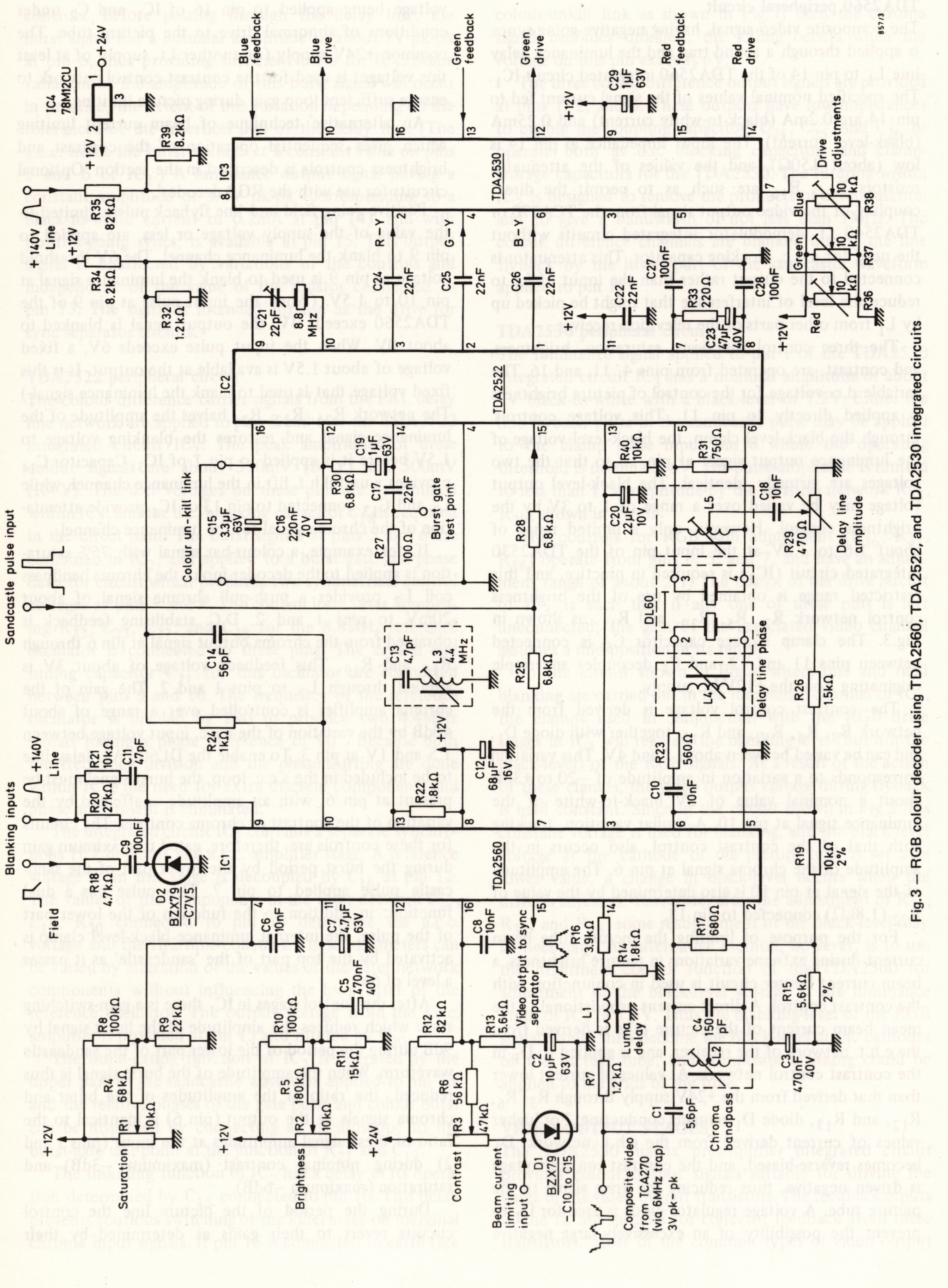
Blue feedback
Blue drive
Green feedback
Green drive
Red feedback
Red drive
IC4 78M12CU
+24V
+12V
R35 82kΩ
R36 8.2kΩ
R34 8.2kΩ
R32 1.2kΩ
+140V Line
IC3
TDA2530
R-Y
G-Y
B-Y
C24 22nF
C25 22nF
C26 22nF
C21 22pF
8.8 MHz
C22 22nF
C27 100nF
C28 100nF
R33 220Ω
C23 47µF 40V
C29 1µF 63V
Drive adjustments
Red
Green
Blue
R36 10kΩ
R37 10kΩ
R38 10kΩ
IC2
TDA2522
C19 1µF 63V
R30 6.8kΩ
C17 22nF
C16 220nF 40V
C15 3.3µF 63V
Colour un-kill link
R27 100Ω
Burst gate test point
R40 10kΩ
R31 750Ω
C20 22µF 10V
L5
C18 10nF
R29 470Ω
Delay line amplitude
R28 6.8kΩ
DL60
Delay line phase
L4
Sandcastle pulse input
C14 56pF
C13 47pF
L3 4.4 MHz
R25 6.8kΩ
R26 1.5kΩ
R24 1kΩ
C12 68µF 16V
R22 1.8kΩ
R23 560Ω
C10 10nF
Blanking inputs
+140V Line
Field
R21 100kΩ
C11 47pF
R20 27kΩ
C9 100nF
R18 4.7kΩ
D2 BZX79 -C7V5
IC1
TDA2560
C6 10nF
C7 4.7µF 63V
C5 470nF 40V
C8 10nF
R16 3.9kΩ
R14 1.8kΩ
R17 680Ω
R19 10kΩ 2%
Video output to sync separator
L1
Luma delay
R8 100kΩ
R9 22kΩ
R10 100kΩ
R11 15kΩ
R12 82kΩ
R13 5.6kΩ
C2 10µF 63V
R7 1.2kΩ
C4 150pF
L2
R15 5.6kΩ 2%
C3 470nF 40V
R4 68kΩ
R1 10kΩ
R5 180kΩ
R2 10kΩ
R6 56kΩ
R3 47kΩ
Saturation
Brightness
Contrast
+12V
+24V
Beam current limiting input
D1 BZX79 -C10 to C15
Composite video from TCA270 (via 6MHz trap) 3V pk-pk
C1 5.6pF
Chroma bandpass
8573

Fig.3 – RGB colour decoder using TDA2560, TDA2522, and TDA2530 integrated circuits

TDA2560 peripheral circuit

The composite video signal, having negative-going syncs, is applied through a sound trap and the luminance delay line L_1 to pin 14 of the TDA2560 integrated circuit IC_1. The specified nominal values of the signal current fed to pin 14 are 0.2mA (black-to-white current) and 0.25mA (black-level current). The input impedance at pin 14 is low (about 150Ω), and the values of the attenuator resistors R_{14}, R_{16} are such as to permit the direct coupling of the video output signal from the TCA270 or TDA2540 i.f. demodulator integrated circuits without the need for a d.c. blocking capacitor. This attenuator is connected to the output rather than the input of L_1 to reduce the level of interference that might be picked up by L_1 from other parts of the television receiver.

The three control functions, saturation, brightness, and contrast, are operated from pins 4, 11, and 16. The variable d.c. voltage for the control of picture brightness is applied directly to pin 11. This voltage controls, through the black-level clamp, the black-level voltage of the luminance output signal at pin 10 so that the two voltages are virtually identical. The black-level output voltage may be varied over a range of 1 to 3V by the brightness control. However, only a limited range of about 1.6 to 1.8V at the input pin of the TDA2530 integrated circuit (IC_3) is required in practice, and this restricted range is obtained by use of the brightness control network R_2, R_5, R_{10}, and R_{11}, as shown in Fig.3. The clamp storage capacitor C_5 is connected between pins 11 and 12, and C_7 decouples any ripple originating from the +12V l.t. supply.

The contrast control voltage is derived from the network R_3, R_6, R_{12}, and R_{13}, together with diode D_1, and can be varied between about 2 and 4V. This variation corresponds to a variation in amplitude of −20 to +3dB about a nominal value of 2V black-to-white of the luminance signal at pin 10. A similar variation, tracking with that of the contrast control, also occurs in the amplitude of the chroma signal at pin 6. The amplitude of the signal at pin 10 is also determined by the value of R_{22} (1.8kΩ) connected to pin 13.

For the purpose of limiting the picture tube beam current during extreme variations in picture brightness, a beam current limiter circuit is used in conjunction with the contrast control. A direct current proportional to the mean beam current of the picture tube is derived from the e.h.t. network of the receiver, and is applied to D_1 in the contrast control network. At values of current lower than that derived from the +24V supply through R_3, R_6, R_{12}, and R_{13}, diode D_1 remains conducting. For higher values of current derived from the e.h.t. network, D_1 becomes reverse-biased, and the contrast control voltage is driven negative, thus reducing the drive signal to the picture tube. A voltage regulator diode is used for D_1 to prevent the possibility of an excessively-large negative voltage being applied to pin 16 of IC_1 and C_2 under conditions of abnormal drive to the picture tube. The common +24V supply (or another l.t. supply of at least this voltage) is used for the contrast control network to ensure sufficient loop gain during picture limiting.

An alternative technique of beam current limiting which gives sequential operation of the contrast and brightness controls is described in the section 'Optional circuits for use with the RGB decoder'.

Positive-going field and line flyback pulses, limited to the value of the supply voltage or less, are applied to pin 9 to blank the luminance channel. The 6V threshold voltage at pin 9 is used to blank the luminance signal at pin 10 to 1.5V. (When the input pulse at pin 9 of the TDA2560 exceeds 3V, the output signal is blanked to about 0V. When the input pulse exceeds 6V, a fixed voltage of about 1.5V is available at the output. It is this fixed voltage that is used to blank the luminance signal.) The network R_{24}, R_{32}, R_{34} halves the amplitude of the luminance signal and restores the blanking voltage to 1.5V before it is applied to pin 1 of IC_3. Capacitor C_{14} provides a useful h.f. lift in the luminance channel, while L_3 and C_{13} connected to pin 13 of IC_1 provide attenuation of the chroma signal for the luminance channel.

If, for example, a colour-bar signal with 75% saturation is applied to the decoder input, the chroma bandpass coil L_2 provides a push-pull chroma signal of about 20mV to pins 1 and 2. D.C. stabilising feedback is obtained from the chroma output signal at pin 6 through R_{15} and R_{19}. This feedback voltage of about 3V is applied through L_2 to pins 1 and 2. The gain of the chroma amplifier is controlled over a range of about 40dB by the variation of the a.c.c. input voltage between 1.5 and 1V at pin 3. To enable the DL60 PAL delay line to be included in the a.c.c. loop, the burst signal must be present at pin 6, with an amplitude unaffected by the variation of the contrast or chroma controls. The circuits for these controls are, therefore, gated to maximum gain during the burst period by the lower part of the sandcastle pulse applied to pin 7. This pulse has a dual function: in addition to the function of the lower part of the pulse, the internal luminance black-level clamp is activated by the top part of the 'sandcastle' as it passes a level of 6V.

After the control stages in IC_1 there is a gain-switching stage which reduces the amplitude of the burst signal by 9dB during the period of the lower part of the sandcastle waveform. When the amplitude of the burst signal is thus reduced, the ratio of the amplitudes of the burst and chroma signals at the output (pin 6) is identical to the ratio of these signal amplitudes at the input (pins 1 and 2) during nominal contrast (maximum −3dB) and saturation (maximum −6dB).

During the period of the picture line the control circuits revert to their gains as determined by their controls. Before passing through the delay line, the burst signal has a nominal amplitude of about 1V pk-pk at pin 6, thus providing sufficient drive for IC_2. Some variation of the amplitude of this burst signal will occur in practice, the extent of this variation depending on the tolerances of the insertion loss of the delay line. (The a.c.c. holds the burst voltage at a constant value on pins 5 and 6 of IC_2.) A luminance output signal having a constant amplitude of 3.4V pk-pk (corresponding to a black-to-white current of 0.2mA at pin 14), and with positive-going syncs, is available at pin 15. This output signal is unaffected by variations of the controls and independent of the value of the resistor connected to pin 13. The signal is intended for use as the drive for sync separator circuits.

TDA2522 peripheral circuit

The colour difference carrier signals from the PAL delay line network are applied to pins 5 and 6 of the TDA2522 integrated circuit IC_2. The peak amplitudes of these colour signals are about 350mV (B–Y) and 500mV (R–Y). The d.c. voltages on these pins are determined within IC_2, and the d.c.-blocking capacitor C_{18} is required in the direct path. The burst signals at pins 5 and 6 are combined in IC_2, and applied to a burst gate and phase detector circuit which produces two symmetrical control voltages at pins 7 and 8. The control loop filter comprising R_{33}, C_{23}, C_{27}, and C_{28} for the 8.8MHz reference oscillator is connected to these pins. The crystal and tuning capacitor C_{21} for this oscillator are connected between pins 9 and 10. The frequency of the reference oscillator is divided by two to produce two 4.4MHz signals having a phase difference of 90°. Because both the frequency division and the phase-shifting are done within IC_2, the need for extra discrete components and phase adjustment is eliminated.

The integrated circuit IC_2 contains a separate synchronous H/2 detector and a.c.c. amplifier stage. A reference voltage from this stage is decoupled by C_{16} at pin 12. The values of the components in the filter network C_{17}, C_{19}, R_{30} connected to pin 14 determine the a.c.c. voltage and the H/2 time-constant. These parameters can be varied by alteration of the values of the filter network components without influencing the loop filter of the reference oscillator. The output voltage from the a.c.c. amplifier is provided at pin 13 and filtered by C_{20}.

The burst-gating function of IC_2 is operated by the upper part of the sandcastle waveform applied to pin 15, and the relative phases of the gate pulse and colour burst can be inspected by connecting an oscilloscope to the burst-gate test point at the junction of R_{27} and C_{17}.

The unkilling function of IC_2 has a delay in its operation determined by C_{15} connected to pin 16. This delay prevents spurious switching of the killer stage on marginal chroma input signals. If pin 16 is connected to earth (see colour-unkill link as shown in Fig.3) then the chroma signal becomes unkilled; the killing occurs when the voltage on this pin exceeds 6V.

The three colour-difference output signals are provided at pins 1, 2, and 3. These outputs have low impedances to enable the coupling capacitors C_{24}, C_{25}, and C_{26} to operate both as d.c. blocking capacitors and clamp-storage capacitors for the TDA2530. The filtering within IC_2 is designed to remove the products of demodulation and to give a bandwidth of not less than 1MHz. The colour difference channels are blanked during the line flyback by the lower part of the sandcastle waveform applied to pin 15.

TDA2530 peripheral circuit

The luminance signal applied to pin 1 of the TDA2530 integrated circuit IC_3 has a nominal amplitude of about 1V black-to-white with a black-level of 1.5V. Either the line flyback pulse or the sandcastle pulse may be applied to the clamp pulse input pin 8 where the operating threshold is nominally 6V. The pulse amplitude is limited to less than 12V amplitude by the resistive network R_{35}, R_{39}, shown in Fig.3.

The controls for RGB gain adjustment (R_{36}, R_{37}, R_{38}) operate from pins 3, 5, and 7, and have an adjustment range of about 2:1. The design of the drive circuit of IC_3 is such that if any one of these pins is left unconnected, the gain of the associated video channel assumes a mid-position in its range.

In the circuit shown in Fig.3, where line and field blanking are carried out in the luminance channel of IC_1, the clamps used in conjunction with the RGB drive stages in IC_3 will regulate the blanking level (but not the black-level) of the RGB signals. As a result of the action of these clamps, the video output voltage during flyback is held constant. Since in the circuit shown in Fig.3 this constant voltage is used for blanking, and the black-level voltage at the cathode of the picture tube is set at a lower value, a change in black-level occurs when the drive is adjusted. Therefore, after the adjustment of R_{36}, R_{37}, and R_{38}, some readjustment of the black-level may be necessary. An alternative method, however, is to use the brightness control function of the TDA2560 for adjustment of the black-level voltage at the luminance input of IC_3 to 1.5V. Thus the blanking-level of the RGB signal would then become the black-level at the cathodes of the picture tube, and composite blanking could be applied to the grids of the tube.

VIDEO OUTPUT STAGES

The TDA2530 matrix preamplifier integrated circuit provides colour output signals suitable for driving the bases of the video output transistors. The feedback inputs of the IC are suitable for collector feedback from these transistors. Most of the common types of video output stage can be used with the TDA2530, three of which are now briefly described. In each description only the blue (B) channel amplifier is shown. The circuits of the red (R) and green (G) channel amplifiers are identical to that of the B channel amplifier, with the exception of certain components common to all three, as indicated. The adjustment of the d.c.-level control, as shown in each type of output stage, is described under 'Alignment procedure'.

Class A single transistor

The circuit of a conventional class A video amplifier, providing overall collector feedback for the TDA2530, is shown in Fig.4. The emitter of TR_1 is biased to 7.5V by voltage regulator diode D_1. The d.c.-level potentiometer R_5 can be adjusted to remove the combined effect of all component tolerances upon the d.c. level of the output signal. During the clamping period, determined by the duration of the clamping pulse at pin 8 of the TDA2530, a voltage of 6V d.c. is set at each of the feedback pins 11, 13, and 15 by the integrated circuit (see Fig.3). The d.c. collector voltage of TR_1 is then determined by the value of the feedback resistor R_3 combined with the values of resistors R_1, R_2, R_4, and R_5 connected from the feedback pin to earth and the +12V supply.

The overall gain of each colour channel, from the luminance input at pin 1 of IC_1 in Fig.3 to the collector of the video output transistor, is determined by the ratio of the feedback resistor R_3 to the equivalent resistance of the network R_1, R_2, R_4, and R_5. It can be seen from Fig.4 that adjustment of R_5 has little effect upon the gain or the frequency response of the output circuit.

The circuit layout, particularly around the feedback resistor R_3, influences the frequency response of the output stage; capacitor C_f can be used in each stage to equalise the frequency response where necessary. This capacitor can take the form of a pad of earthed copper on the printed-wiring board immediately under R_3. The size and shape of this pad must be determined experimentally to achieve the desired response.

Class AB push-pull

The circuit of a typical class AB push-pull amplifier using complementary transistors, types BF422 and BF423, biased with finite quiescent current, is shown in Fig.5. A detailed description of this type of circuit has been given elsewhere (Ref.2). Although class B and AB amplifiers require more components than single-transistor class A types, they offer a substantial reduction in power dissipation and better transient response. In addition, a saving in h.t. supply of about 10 to 20V is possible for a given output voltage requirement. Each video output stage is connected as part of the associated feedback loop to define the stage gain: this ensures good d.c. stability and identical a.c. performance of the three stages.

The bias for TR_2 is provided by the voltage regulator diode D_1 (common to the three output stages), and for TR_1 by resistors R_1, R_2, and R_3. Resistor R_7 and capacitor C_2 enable TR_1 to have a high but defined gain. Resistor R_8 reduces the power dissipation in TR_1. The feedback resistor R_{11} and the network R_9, R_{10} define the overall gain of the stage (100 times), and R_{12} and R_{13} determine the d.c. output voltage of the stage.

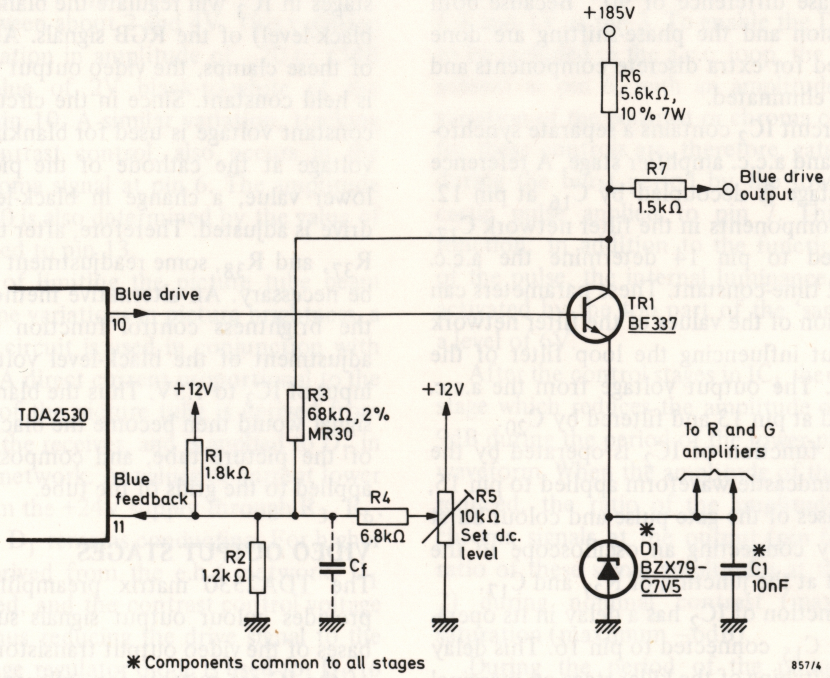

Fig.4 – Class A video output stage

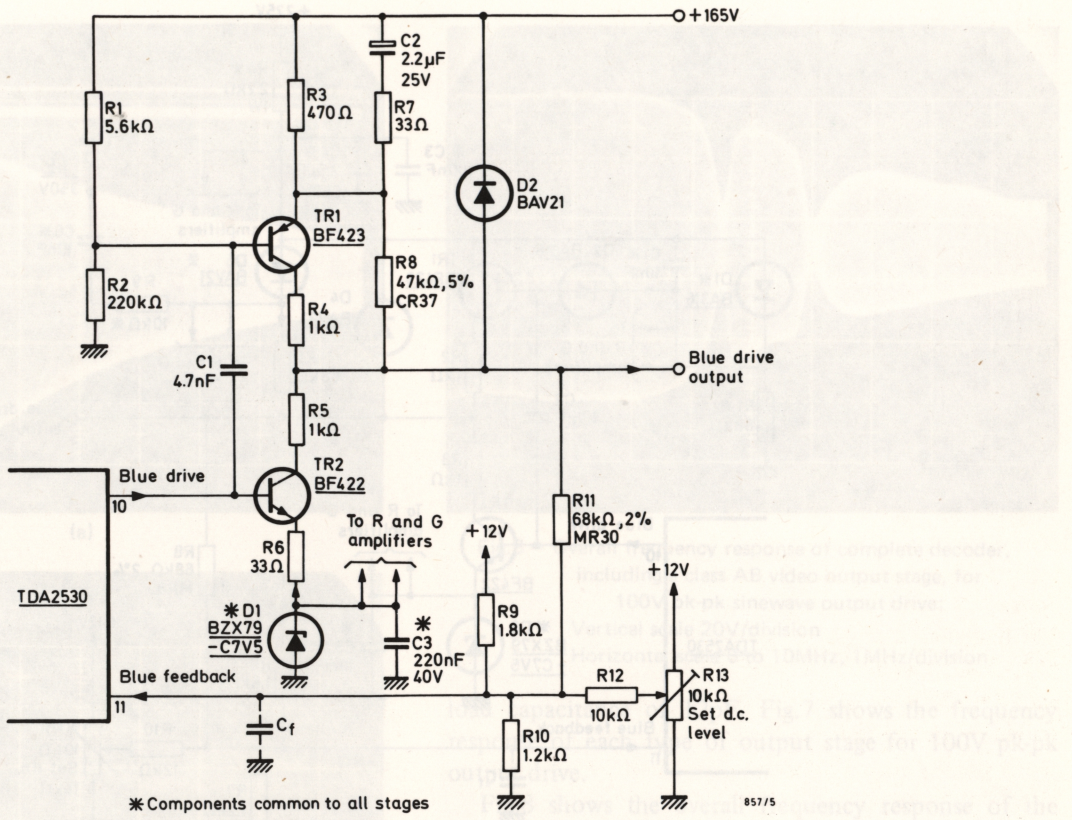

Fig.5 – Class AB complementary push-pull video output stage

The inclusion of capacitor C_f (having a value of about 10pF) in the feedback network may be necessary to compensate for the effects of variations in the circuit layout of the three stages, or possibly for the parallel capacitance of a given type of feedback resistor. The addition of C_f to the circuit in the position shown in Fig.5 compensates for a *falling* video response of the output stage, determined by a particular component layout. With a different layout, however, the circuit might have a *rising* video response which would require additional capacitance in parallel with the feedback resistor to achieve the correct type of compensation. Both types of compensation can be accomplished by the provision of a pad of copper on the printed-wiring board under R_{11}, the pad being connected to earth or to one end of the resistor.

With an h.t. supply of 165V, and with the black-level adjusted by R_{13} to 130V, the total power dissipation in each stage is about 1W. The highest power dissipation occurs under h.f. overdrive conditions (for example, with a 5MHz continuous grating applied to the luminance input of the TDA2530), when the power dissipation can increase to a level corresponding to about 530mW in TR_1 and 570mW in TR_2. These figures assume a load capacitance of 12pF on each stage. The ratings of the BF422 and BF423 transistors are such that the heat from TR_1 and TR_2 can be dissipated from the copper of the printed-wiring board. A pad of copper $100mm^2$, to which the collector is attached, provides an adequate heatsink for each transistor.

Diode D_2 provides protection against flashover discharges in the picture tube. Flashover tests carried out on this type of circuit in a practical tv receiver have not revealed any inherent weaknesses in the circuit design.

Class B push-pull

A class B video amplifier can be designed to have zero quiescent current in the transistors, thus minimising power dissipation. However, a line flyback pulse must be applied to this type of circuit to maintain true class B operation under all signal conditions.

A typical class B amplifier circuit is shown in Fig.6. The current consumption of this circuit varies in accordance with the video h.f. content of the input drive signal: the minimum current is 10mA and the maximum current is 20mA. The maximum dissipation of TR_1 and TR_2 is limited by means of resistor R_4 in series with the 225V supply to the video output stages. Because practical tv pictures may contain h.f. information during parts of each field, the supply on the low-voltage side of this resistor is filtered sufficiently to prevent load variations at field rate. Any variations of h.t. supply voltage will, however, have minimal effect on the picture tube drive voltages because of the clamped feedback configuration

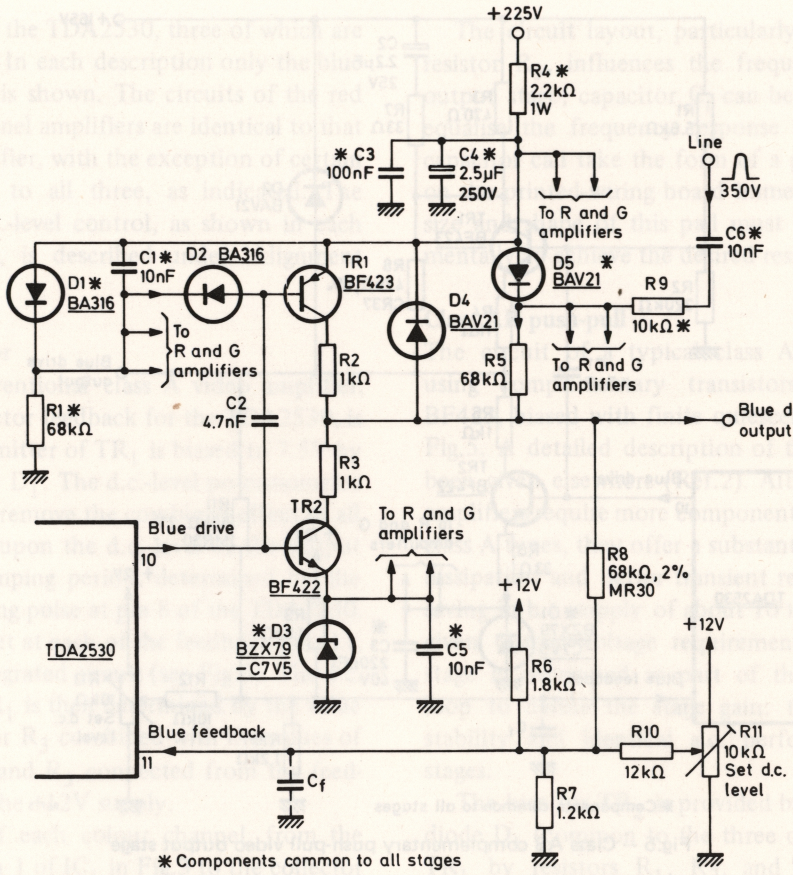

Fig.6 – Class B complementary push-pull video output stage

of the output stage. The two 1kΩ resistors between the collectors of the output transistors and the video output reduce the collector dissipation during signal transients with little sacrifice of output voltage swing. To minimise the dissipation in both output transistors, resistor R_5, equal in value to the feedback resistor R_8, is connected in series with diode D_5 between the supply and the video output.

Positive output current, charging the capacitance presented by the picture tube, will flow by conduction of TR_1. Transistor TR_1 receives its drive through the base coupling capacitor C_2, which will itself become charged. To discharge C_2, the flyback pulse is applied through C_6, R_9, and R_5 to the output, and causes TR_2 to conduct by the action of the feedback loop. At the same time, TR_1 ceases conduction, and C_2 discharges through D_2 into the network consisting of D_1, C_1, and R_1. The small biasing voltage at the cathode of D_1 minimises crossover effects.

Video response

Each of the three types of video output stage just described is designed to provide adequate drive for full performance of 20AX picture tubes. Table 1 summarises the frequency response (to –3dB) of each type of output stage. The figures shown in Table 1 are applicable for a load capacitance of 12pF. Fig.7 shows the frequency response of each type of output stage for 100V pk-pk output drive.

TABLE 1

Frequency Response of Video Output Stages shown in Figs.4, 5, and 6

Maximum output voltage (V pk-pk)	Frequency response Class A (Fig.4) (MHz)	Class AB (Fig.5) (MHz)	Class B (Fig.6) (MHz)
100	4.5	5.6	5.6
40	7	9	9

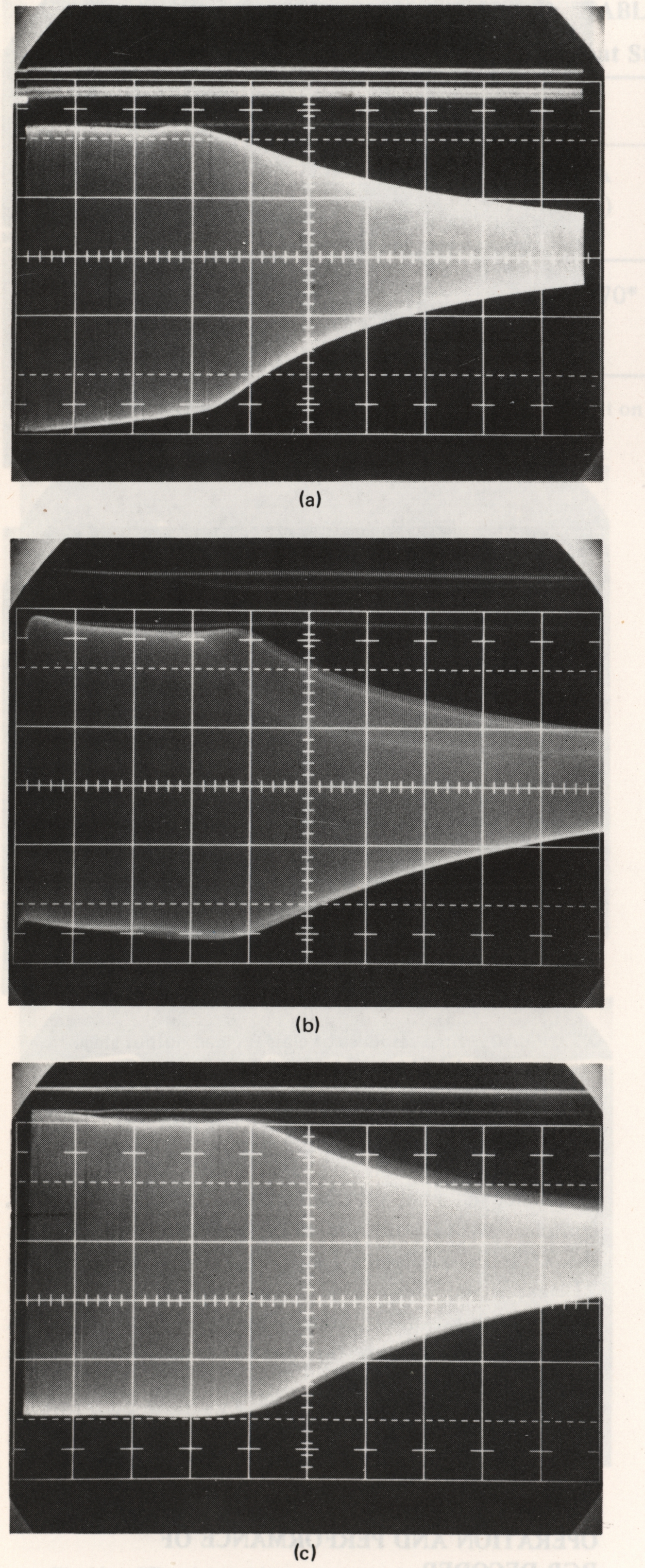

Fig.7 – Frequency response of video output stages for 100V pk-pk sinewave output drive:
(a) class A, (b) class AB, (c) class B.
Vertical scale 20V/division
Horizontal scale 0 to 10MHz, 1MHz/division

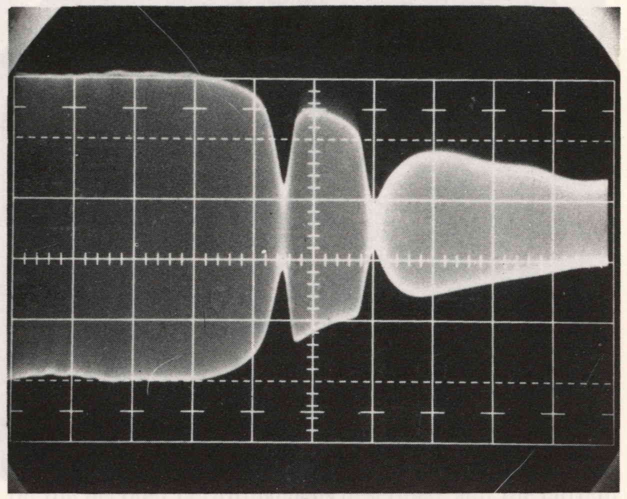

Fig.8 – Overall frequency response of complete decoder, including a class AB video output stage, for 100V pk-pk sinewave output drive:
Vertical scale 20V/division
Horizontal scale 0 to 10MHz, 1MHz/division

Fig.8 shows the overall frequency response of the RGB decoder, including a sound trap and a class AB video output stage. It can be seen from Fig.8 that there is a considerable response in amplitude between 4.4 and 6MHz, and that this is limited by the frequency response of the video output stage. In a practical tv receiver, however, video frequencies above 4MHz are attenuated by the slope of the i.f. frequency response, and it is the i.f. amplifier that will determine the overall video frequency response of the receiver.

Step-responses of the complementary output stages are symmetrical, even at high drive voltages, whereas the class A output stage has an asymmetrical response at high drive voltages, becoming symmetrical at low drive voltages. The results of measurements of step-response for the circuits shown in Figs.4, 5, and 6 are given in Table 2.

The asymmetry of the class A response at high drive voltages arises from the inability of the collector load resistor to supply sufficient current to the capacitive load at voltages approaching the h.t. value. Under these conditions no benefit can be obtained from the feedback, because the output transistor is fully cut off. The complementary output stage, however, has a symmetrical response under normal operating conditions, independent of the drive voltage. This symmetrical response results in equal rise-times and fall-times of the output waveform. The waveforms of step-response shown in Figs.9 and 10 for the class A and class B amplifiers illustrate these points.

A 2T pulse-and-bar test carried out on the complete

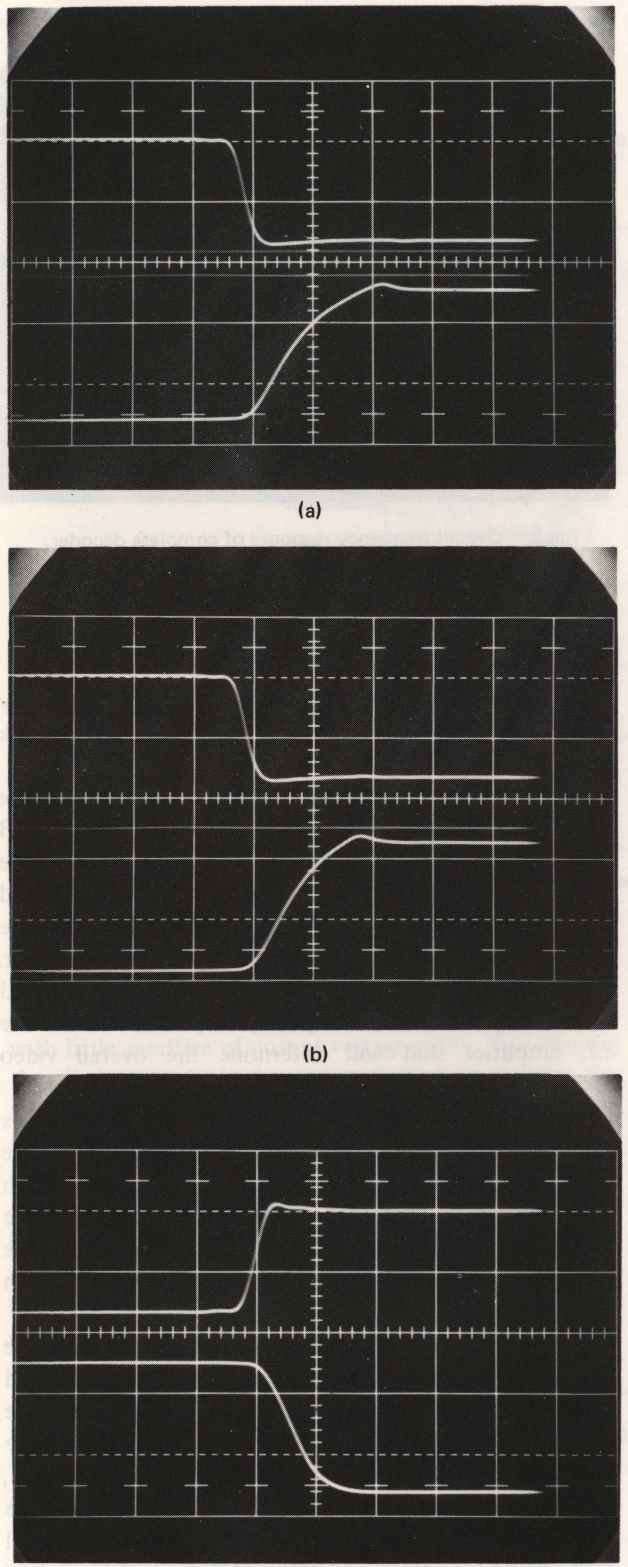

Fig.9 – Step-response of class A video output stage:
(a) white-to-black,
(b) white-to-black with higher brightness,
(c) black-to-white.
Upper trace input voltage, lower trace output voltage,
Vertical scale 50V/division (lower trace only)
Horizontal scale 100ns/division

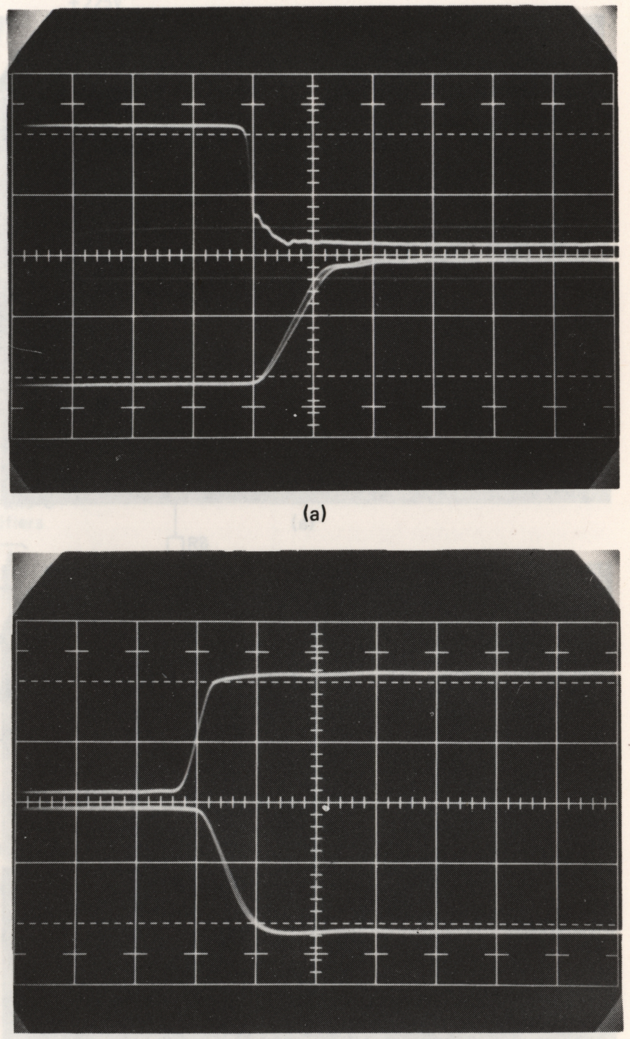

Fig.10 – Step-response of class B video output stage:
(a) white-to-black, (b) black-to-white.
Upper trace input voltage, lower trace output voltage.
Vertical scale 50V/division (lower trace only)
Horizontal scale 100ns/division

luminance channel of a laboratory prototype decoder, complete with its chroma and sound traps, showed that the K factor is between 1 and 2%. (The pulse part of the 2T test signal consists of a $\sin^2$ pulse having a half-amplitude duration of 200ns.) The addition of the class A output stage increases this factor to about 4% at the highest drive voltages.

Fig.11 shows the 2T pulse-and-bar response for the complete luminance channel including a complementary class AB output stage.

OPERATION AND PERFORMANCE OF RGB DECODER

The operation and performance of the RGB decoder is now considered, with regard in particular to the influence of the picture controls on the output voltages. The influence of variations in the l.t. and h.t. supply voltages on the decoder performance is described, and the current consumption of the decoder is derived. Two methods of voltage regulation for the l.t. supply of the decoder alone, and for the whole receiver, are also described.

TABLE 2

Step-response of Video Output Stages shown in Figs.4, 5, and 6

	Step-response		
	Class A (Fig.4) (μs)	Class AB (Fig.5) (μs)	Class B (Fig.6) (μs)
Rise-time (W–B)	140 to 170*	100	100
Fall-time (B–W)	110	100	100

*Rise-time dependent on setting of brightness control

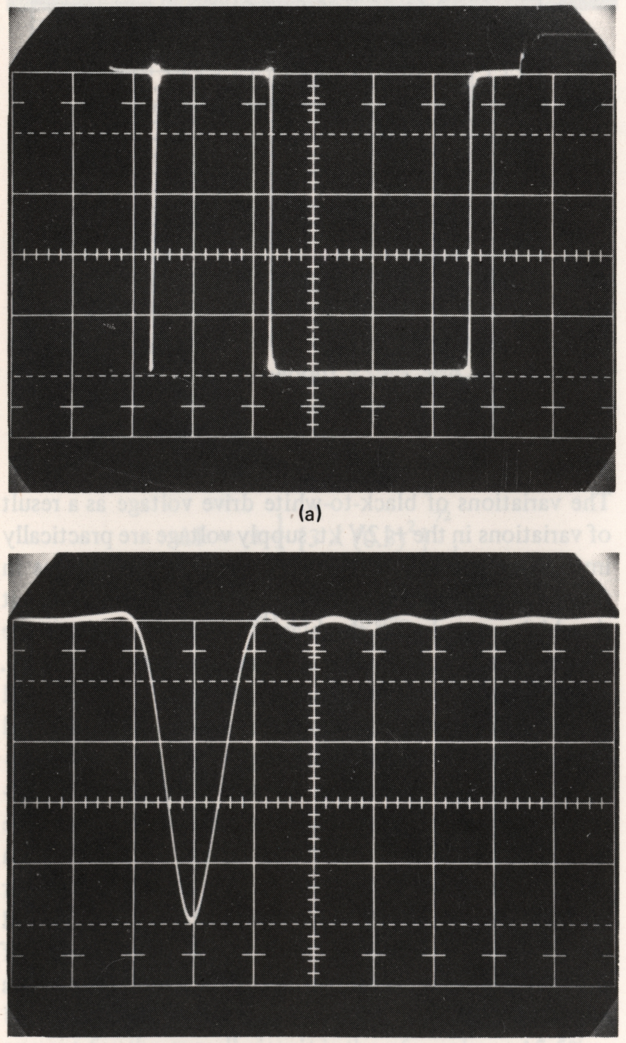

Fig.11 – 2T pulse-and-bar response of complete decoder including class AB complementary output stage:
(a) complete tv line of pulse-and-bar signal,
(b) pulse part of waveform.
Vertical scale 20V/division
Horizontal scale 200ns/division (trace b only)

Picture controls

The picture controls R_1 (saturation), R_2 (brightness), and R_3 (contrast) are shown in Fig.3. The circuit is arranged so that the resistance tolerance of these controls (generally about ±20%) has little effect upon the final control voltages applied to IC_1. A minimum of interconnecting leads for the picture controls has been used in the general circuit of the decoder shown in Fig.3. An advantage of the control circuit is that a picture may be displayed with the three controls disconnected from the circuit.

Fig.12 shows the linear variation of the luma signal amplitude at pin 10 of IC_1 with the variation of the

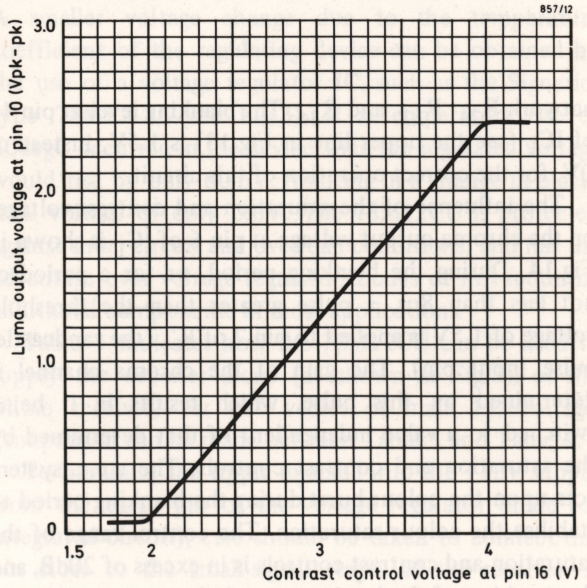

Fig.12 – Contrast control of luma output signal (black-to-white) for TDA2560 integrated circuit

contrast control voltage at pin 16. At nominal contrast (that is, −3dB from the maximum signal at pin 10) the black-to-white output voltage at pin 10 is 2V pk-pk. The input signal at pin 14 required for this output is 0.2mA black-to-white current, with a value of 1.8kΩ for R_{22} (connected between pin 13 and the +12V supply). The spread of the luma output voltage at pin 10 under these circumstances is from 1.7 to 2.3V black-to-white.

The operation of the brightness control is shown in Fig.13, in which the voltage at pin 11 of IC_1 is related to the black-level of the luma signal at pin 10. The linear behaviour and the close tracking of these two voltages is evident from the two lines. The lower line shows the variation of black-level at pin 1 of IC_3 after the resistor network R_{24}, R_{32}, and R_{34}. The blanking level at pin 10 of IC_1 (see the upper line in Fig.13) is 1.5V, instead of 0V, for the correct operation of this circuit.

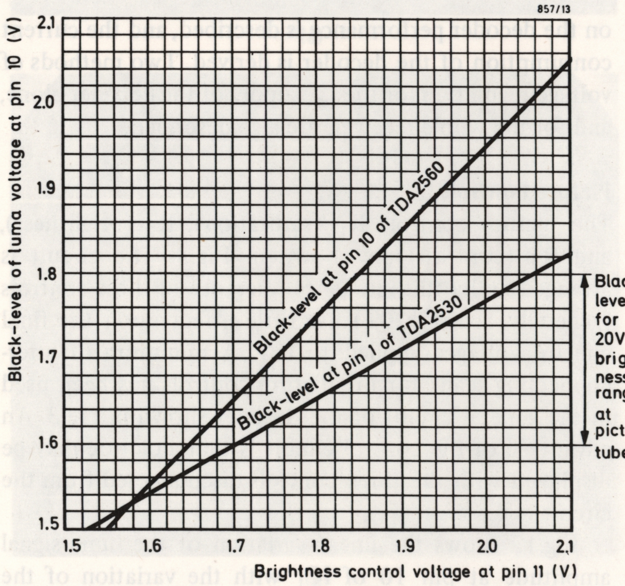

Fig.13 – Brightness control of luma output signal (black-level) for TDA2560 integrated circuit

The influence of the saturation and contrast voltages on the chroma output voltage at pin 6 of IC_1 is shown in Fig.14. During the blanking period, or for a period of not less than 8μs, a pulse greater than the threshold voltage of 1.5V is applied to pin 7 of IC_1 (the sandcastle-pulse input pin). The gain of the chroma channel is determined by this pulse, which results in it being switched to a value independent of that determined by the saturation and contrast controls. The a.c.c. system acts upon the colour burst during the blanking period to stabilise the colour saturation. The control range of the saturation and contrast controls is in excess of 20dB, and the tracking of the luminance and chroma gain is better than 2dB for a control variation of 10dB.

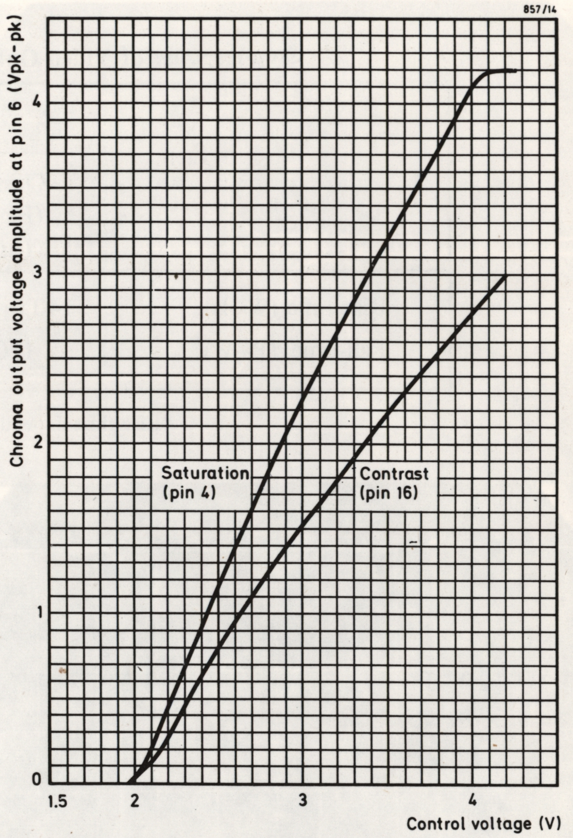

Fig.14 – Control of chroma amplitude by the contrast and saturation control voltages

Effects of variations in +12V l.t. supply

The variations of black-to-white drive voltage as a result of variations in the +12V l.t. supply voltage are practically immeasurable. The colour difference signal changes in proportion to changes in the +12V supply, although it should be noted that the black-to-white drive from the i.f. and demodulator stages is influenced in the same way. Thus if the decoder and i.f. amplifier are both operated from the same supply, then the saturation is unaffected by variations in this common supply.

For a change of 0.5V in the +12V supply, the black-level voltage changes by approximately 5V when the nominal black-level is 140V. The extent of this variation is determined by the feedback circuit of IC_3. If a power supply derived from a voltage regulator diode is used, and the diode has a voltage tolerance of 5%, then a spread of ±6V in the black-level voltage may result from this tolerance.

Effects of variations in h.t. supply

Because of the high loop gain of the d.c.-clamped feedback, the influence of variations in the h.t. supply on the black-level is negligible. Fig.15 shows a ripple voltage of 20V pk-pk at 100Hz superimposed on the h.t. supply (upper trace), and the effect of this ripple on the black-level voltage (lower trace).

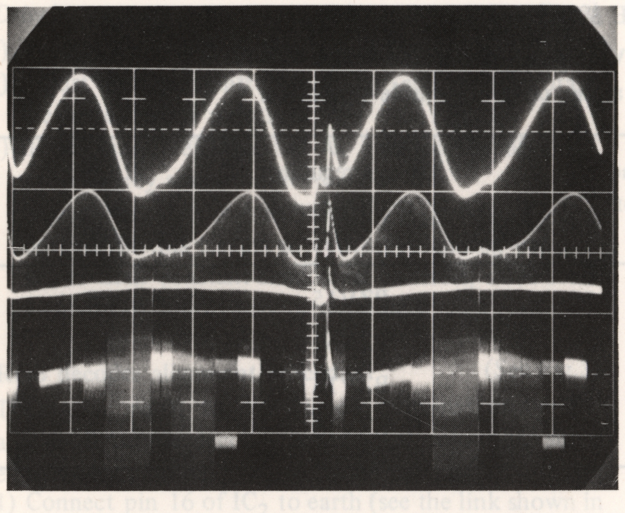

Fig.15 – Top trace: 20V pk-pk 100Hz ripple superimposed on h.t. supply
Lower traces: effect of this ripple on the black-level voltage

Current consumption

The l.t. current consumption of the decoder is about 170mA, of which 150mA is drawn by the integrated circuits. The spread of the current consumption of any one integrated circuit is about ±30%, and therefore, for the TDA2560, TDA2522, TDA2530 combination, the spread in current ΔI is given by:

$$\Delta I = \pm\frac{1}{3}\left[3 \times (0.3)^2\right]^{1/2},$$

$$= \frac{\pm 0.3}{\sqrt{3}} = \frac{\pm 30\%}{\sqrt{3}},$$

or: $$\Delta I \simeq \pm 17.3\%,$$

assuming that the nominal current for each device is about the same.

Thus the expected spread in the total current consumption of the overall circuit of the RGB decoder is:

$$\left[(0.173 \times 150)^2 + (0.1 \times 20)^2\right]^{1/2} \simeq 26\text{mA},$$

assuming a spread of 10% in the current drawn by the bias networks and control circuits. The total spread in current for the overall circuit is therefore about 15.5%.

An l.t. current consumption of 200mA is assumed as being the maximum current of the decoder for the remainder of this article.

The h.t. current consumption depends on the type of video output stage in use, and also to some extent on the picture content. For a typical picture, and normal settings of the controls, the current consumption of each type of video output stage is:

class A	30 to 40mA,
class AB	18 to 20mA,
class B	10 to 20mA.

Typically, the maximum h.t. current consumptions of these output stages are:

class A (bottomed)	95mA,
class AB (3MHz sinewave or noise)	25mA,
class B (4MHz sinewave or noise)	30mA.

Power supplies

The l.t. current consumption of the whole tv receiver should be taken into account when designing the l.t. supply circuit, because it is convenient to supply all parts of the tv circuit requiring +12V from the same source.

The total current consumption from the +12V supply of a receiver using TCA270, TBA120S or TBA750, TBA920, TDA2560, TDA2522, and TDA2530 integrated circuits is about 330mA. The expected spread of this current is ±15%, derived from statistical addition of the individual spreads of current of all the integrated circuits.

Voltage regulator diode

Examples of the components required for simple voltage-regulating networks for the l.t. supplies of the decoder alone or the whole receiver, for two values of main l.t. voltage, are given in Table 3.

If the junction temperature of the voltage regulator diode rises by 60degC during warm-up, the regulated voltage will rise by 0.6V as a result of the temperature coefficient of the diode. This increase in voltage would result in a change in black-level voltage of about 6V (see under 'Black-level').

Voltage regulator IC

A smaller voltage change due to the temperature coefficient of the regulating device can be obtained by the use of a voltage regulator IC, such as the Signetics type 78M12CU (see Fig.3). If a temperature rise of 60degC occurred in the device, then the regulated voltage would rise by only 60mV, resulting in a change in black-level voltage of only 0.6V. The 78M12CU is protected against short-circuit and overload conditions, and has the advantage over voltage regulator diodes of not requiring additional components in most applications.

Table 4 indicates how the 78M12CU can be used to supply the decoder alone (as shown in Fig.3), or the whole receiver, for two values of main l.t. voltage. Comparison can be made between Table 3 and Table 4.

To minimise the ripple injected into the +12V supply from the earth pin of the voltage regulator diode (or integrated circuit), care should be taken to connect this pin close to the small-signal stages of the receiver. A convenient position for the voltage-regulating device is the printed-wiring board of the RGB decoder.

TABLE 3

Component Values for Simple Voltage-regulating Networks for l.t. supplies of the RGB decoder alone, or of the whole tv receiver

	Source voltage (V)	Series-connected resistor (Ω)	Voltage regulator diode	P_z max (W)
Decoder alone	24	47	BZV15	1.9
	16	18	BZX61	1.2
Whole receiver	24	27	BZV15	3
	16	10	BZV15	2.4

TABLE 4

Component Values for 78M12CU Voltage Regulator IC for l.t. supplies of the RGB decoder alone, or of the whole tv receiver

	Source voltage (V)	Series-connected resistor (Ω)	Heatsink required (degC/W)
Decoder alone	24	None	20
	16	None	None
Whole receiver	24	None	8
	24	18	22
	16	None	40
	16	2	None

ALIGNMENT PROCEDURE

Apart from the adjustments for the picture tube drive, only five adjustments are required in the decoder.

1) Reference oscillator: adjustment of free-run frequency
2) Delay line: phase adjustment
3) Delay line: amplitude adjustment
4) Chrominance input filter: frequency adjustment
5) 4.4MHz trap in luminance channel: limitation of patterning on coloured areas.

If a suitable line oscillator circuit is used, such as a circuit using the TDA2590 or TDA2571 integrated circuits, the correct timing of the burst-gate and black-level clamp pulses will be obtained without the need for any adjustment. If such a circuit is not available, then the circuit shown in Fig.16 will be required after the line oscillator to generate a sandcastle pulse from the line flyback pulse; one further adjustment will then be necessary. The operation of the circuit shown in Fig.16 is described under 'Optional circuits for use with the RGB decoder'.

Picture tube drive adjustments

The adjustments required for each colour channel are first to the cut-off point of the picture tube, and second to the drive signal.

Cut-off

(See classes A, AB, and B output stages shown in Figs.4, 5, and 6)

1) While observing the R, G, and B drive waveforms in turn by connecting an oscilloscope to the cathodes of the picture tube, adjust the d.c.-level potentiometers of the video output stages so that the drive voltage during flyback is 165V for class A and class B stages, or 150V for class AB stages.
2) With a blank raster (black) signal applied to the decoder, adjust the brightness control to obtain a black-level voltage at the cathodes of the picture tube of 145V for class A and class B stages, or 130V for class AB stages. The A_1 (G_2) controls should then be adjusted to obtain raster cut-off.

Drive (See Fig.3)

1) Apply a grey-scale signal to the decoder.
2) Adjust the drive controls R_{36}, R_{37}, and R_{38} to obtain the correct white point.
3) If necessary, readjust the A_1 controls to obtain a uniform grey scale.
(Note: Because the drive controls R_{36}, R_{37}, and R_{38} operate in this circuit as constant-blanking controls rather than constant-black-level controls, some readjustment of cut-off may be required.)

RGB decoder alignment procedure (See Fig.3)

The input signal to the decoder required during the alignment of the decoder is a normal colour-bar signal except where stated.

1) Connect pin 16 of IC_2 to earth (see the link shown in Fig.3) to unkill the chroma channel.
2) Adjust the delay line amplitude control R_{29} to its maximum setting.
3) Adjust the picture controls until colours are displayed on the tv screen. Rough adjustment of the chroma bandpass coil L_2 may also be required.
4) Unless the reference oscillator is to be adjusted (the next stage in the alignment procedure), remove the link between pin 16 and earth.

Reference oscillator

1) Connect the link between pin 16 of IC_2 and earth.
2) Short-circuit pins 5 and 6 of IC_2 to disable the phase detector.
3) Adjust trimmer capacitor C_{21} until the rolling of the colours ceases.
4) Remove the short-circuit from pins 5 and 6, allowing the oscillator to lock.
5) Remove the link between pin 16 and earth.

Adjustment of sandcastle pulse timing

The adjustment procedure given below will only be required where it has been necessary to use the circuit shown in Fig.16 with the existing line oscillator to generate sandcastle pulses of the correct timing. The adjustment should be carried out in conjunction with that of the subcarrier reference oscillator.

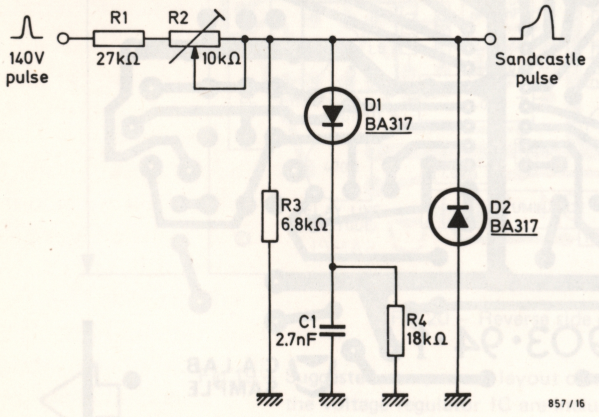

Fig.16 – Circuit used for generation of a sandcastle pulse from the line pulse

If potentiometer R_2 in Fig.16 is adjusted for minimum resistance, then the burst-gate pulse width will be excessively large but the reference oscillator will be able to lock. After the subcarrier lock is achieved, the following procedure can be carried out.

1) Observe with an oscilloscope the waveform across R_{27}. This waveform will consist of the demodulated colour burst, and the burst part should appear within the gated period, as shown in Fig.17.
2) Adjust R_2 (Fig.16) until the burst pulse is just contained within the gating period. (The width of the gating period should be about 5μs, as shown in Fig.18.) Excessive saturation will occur if the burst is partly cut off by the gate. (The a.c.c. operation is

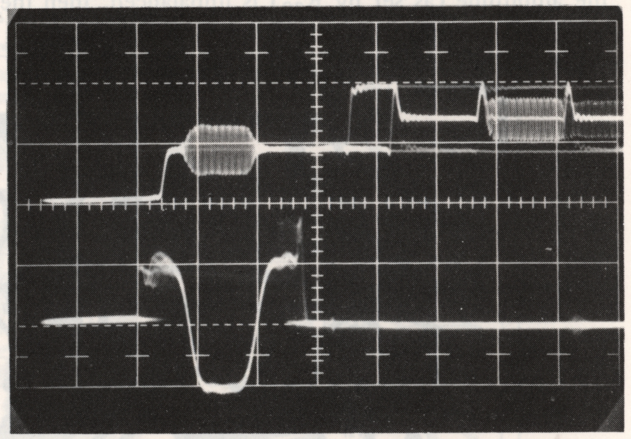

Fig.17 – Demodulated colour-burst waveform at burst-gate test point of R_{27} in Fig.3.
Upper trace: part of composite video signal containing colour information
Lower trace: demodulated colour-burst waveform
Vertical scale 5mV/division
Horizontal scale 2μs/division

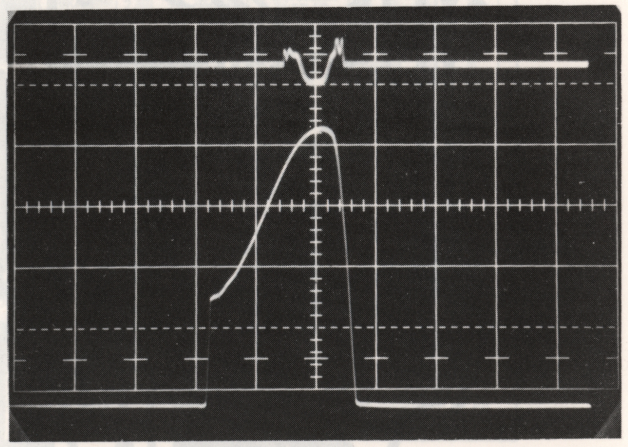

Fig.18 – Sandcastle pulse (lower trace) provided by circuit shown in Fig.16, and demodulated colour-burst waveform (upper trace), as measured at the burst-gate test point of R_{27} in Fig.3.
Vertical scale 2V/division (lower trace only)
Horizontal scale 5μs/division

dependent on the gate width, and the amplitude of the chroma output signal also increases as the gate widens.) Therefore, care should be taken to ensure that the gate is correctly positioned and of the correct width.

Delay line (See Fig.3)

A special test pattern containing B–Y signals alternating from line-to-line, and non-alternating R–Y signals, is required for the alignment of the delay line. Pattern generators types PM5544 and PM5509 (N.V. Philips) can both be used to generate this pattern.

The phase of the delay line is adjusted by L_4 and the amplitude is adjusted by R_{29}. When both controls are correctly adjusted, no output signal will be produced by the delay line in either the B–Y or the R–Y channel. If the amplitude (as set by R_{29}) is unbalanced, then the signals present in both channels will result in the display of Hanover bars. Because an unbalance in the delay line signal becomes apparent only when the burst phase is incorrect, the alternative method of amplitude adjustment using normal colour-bar patterns (see Ref.1) is not described here. The burst phase of the RGB decoder cannot be easily maladjusted to reveal such unbalance.

Chrominance input filter

Two methods for alignment of the chroma bandpass coil L_2 are described below. Either of these methods may be used.

Method 1

1) With an oscilloscope connected to pins 1, 2, or 3 of IC_2, observe the waveform displayed.
2) Adjust L_2 for optimum transient response.

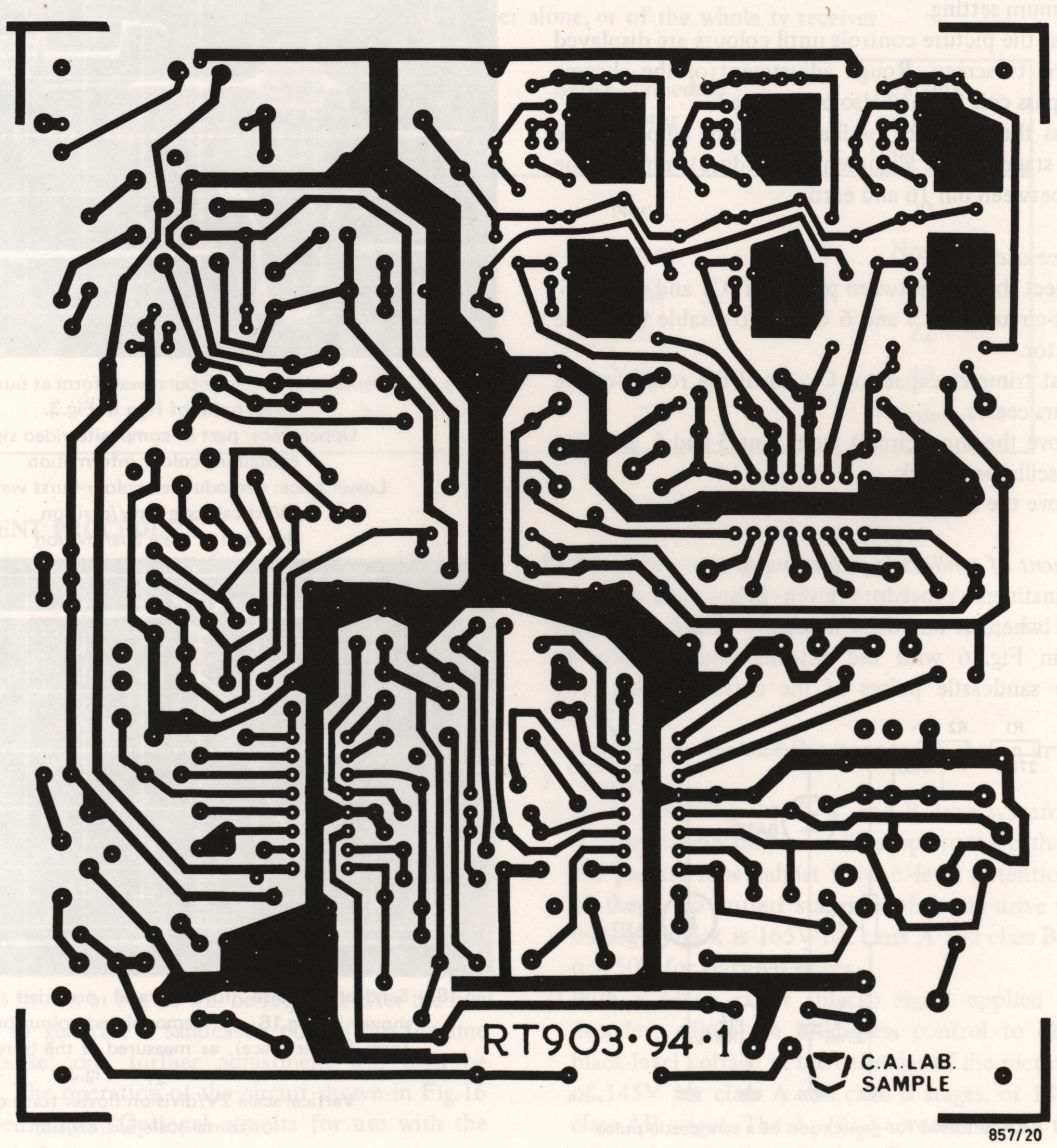
RT903·94·1
C.A.LAB
SAMPLE
857/20

Fig.20 — Reverse side of printed-wiring board

Method 2

1) With an oscilloscope or a high-impedance electronic voltmeter connected to pin 13 of IC_2, observe the a.c.c. voltage.
2) Adjust L_2 for minimum a.c.c. voltage.

(Note: Method 2 is easier to carry out if the burst amplitude of the pattern generator is reduced towards the point at which colour-killing occurs.)

4.4MHz luminance trap

1) Adjust the saturation control R_1 to zero.
2) Adjust the luminance trap L_3 for minimum patterning in bulk coloured areas; that is, away from the edges of the colour-bar test signal.

Some patterning near the transient parts of colour bars is inevitable; the trap is designed to have a response that is a good compromise between transient response and impairment of luminance bandwidth.

PRINTED-WIRING BOARD COMPONENT LAYOUT

A suggested layout of the components on the printed-wiring board for the decoder, including class AB video output stages (see Fig.5) and the 78M12CU voltage regulator IC, is shown in Fig.19. Most of the circuits described under 'Optional circuits for use with the RGB decoder' have been included on the board. Space has also been provided for a sound trap (an example of which is described later), but this trap is often situated on the i.f. board. The reverse side of the board is shown in Fig.20.

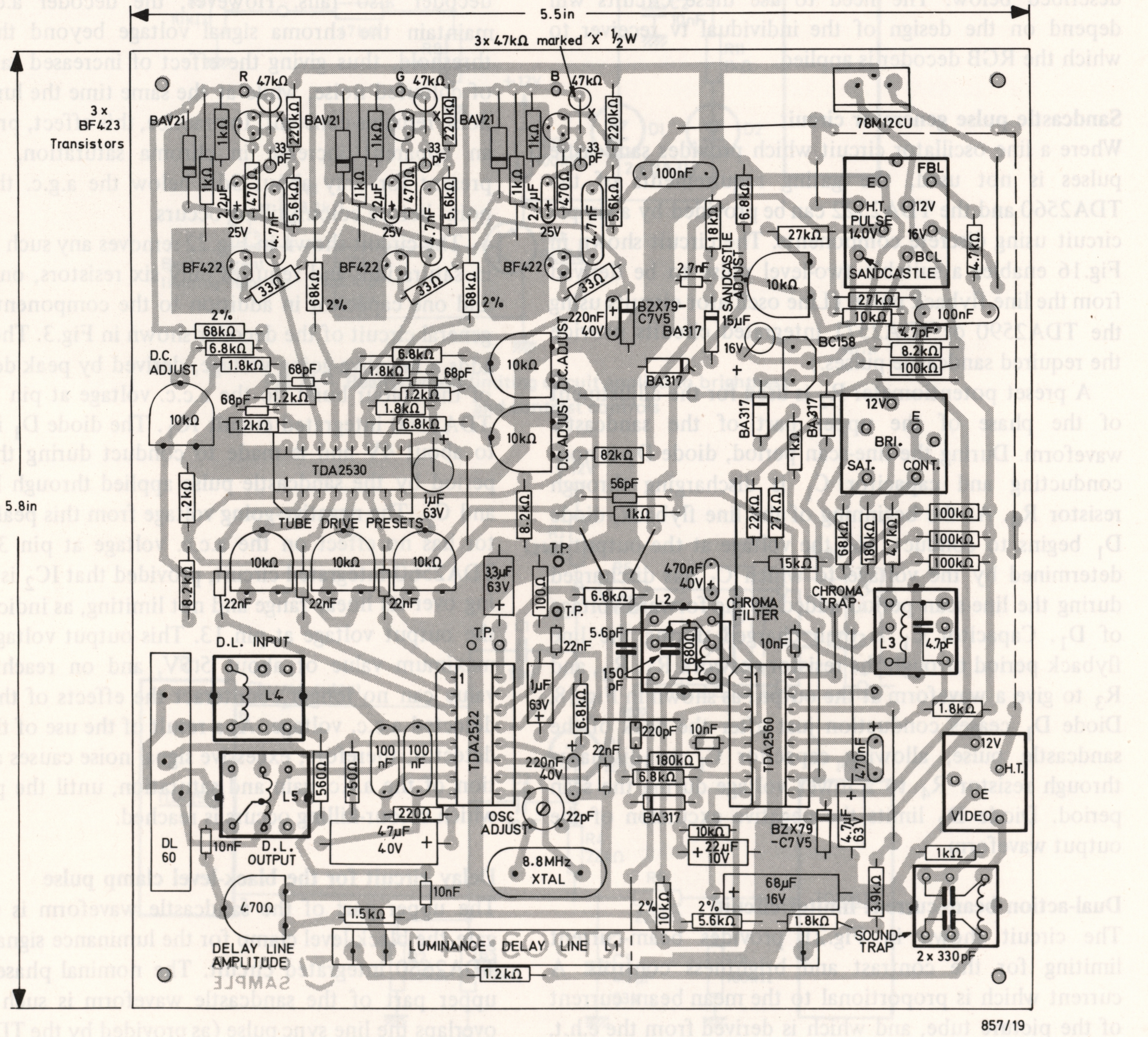
5.5in
3x 47kΩ marked 'X' ½W
5.8in
R
G
B
3x BF423 Transistors
BAV21
BF422
78M12CU
EO
FBL
O.H.T. PULSE 140V
12V
16V
BCL
SANDCASTLE
BC158
BZX79-C7V5
BA317
D.C. ADJUST
TDA2530
TUBE DRIVE PRESETS
T.P.
D.L. INPUT
L4
L5
DL 60
D.L. OUTPUT
DELAY LINE AMPLITUDE
LUMINANCE DELAY LINE L1
TDA2522
OSC ADJUST
8.8MHz XTAL
L2
CHROMA FILTER
CHROMA TRAP
L3
TDA2560
12V
BRI.
SAT.
CONT.
O.H.T.
OE
VIDEO
SOUND TRAP
2x 330pF
857/19

Fig.19 — Suggested component layout of the RGB decoder printed-wiring board. The class AB output stages and the voltage regulator IC are included on the board, together with most of the optional circuits; namely, the sandcastle pulse generator, the beam-current limiter, the delay circuit for the black-level clamp pulse, and the sound trap

In the section 'Video output stages', the provision of extra printed copper under the feedback resistors to achieve the correct video compensation is described. The requirement for such compensation may be kept to a minimum if the unwanted parasitic capacitances resulting from the initial layout of the printed-wiring board are small in value. In a compact board layout, this requirement applies particularly to the capacitance between the printed copper heatsink of each class AB or B transistor and the track connected directly to the feedback pins 11, 13, and 15 of the TDA2530.

OPTIONAL CIRCUITS FOR USE WITH THE RGB DECODER

Five optional circuits which can be used in conjunction with the general circuit of the decoder (Fig.3) are described below. The need to use these circuits will depend on the design of the individual tv receiver to which the RGB decoder is applied.

Sandcastle pulse generator circuit

Where a line oscillator circuit which provides sandcastle pulses is not used, the gating requirements of the TDA2560 and the TDA2522 can be provided by a simple circuit using discrete components. The circuit shown in Fig.16 enables a suitable two-level pulse to be derived from the line flyback pulse. (Line oscillator circuits using the TDA2590 or TDA2571 integrated circuits provide the required sandcastle pulses.)

A preset potentiometer R_2 is used for the adjustment of the phase of the upper part of the sandcastle waveform. During the line-scan period, diode D_1 is non-conducting and capacitor C_1 is discharging through resistor R_4. At the beginning of the line flyback, diode D_1 begins to conduct, and the voltage at the output is determined by the voltage to which C_1 has discharged during the line-scan period added to the forward voltage of D_1. Capacitor C_1 is then charged during the line flyback period through the resistor network R_1, R_2, and R_3 to give a waveform at the output as shown in Fig.18. Diode D_1 ceases conduction just after the peak of the sandcastle pulse, allowing capacitor C_1 to discharge through resistor R_4 to a lower voltage during the scan period. Diode D_2 limits the negative excursion of the output waveform.

Dual-action beam-current limiter circuit

The circuit shown in Fig.21 provides beam-current limiting for the contrast and brightness controls. A current which is proportional to the mean beam current of the picture tube, and which is derived from the e.h.t. circuit, is applied as shown in Fig.21. Increasing beam current drives the voltage at the base of TR_1 negative towards 0V. The anode voltages of diodes D_1 and D_2 are equal to the d.c. voltages at the brightness and contrast control pins of IC_1. As the emitter voltage of TR_1 is reduced by increasing beam current, diode D_1 will conduct before D_2 conducts because the nominal contrast control voltage is 3V and the nominal brightness control voltage is about 1.8V. The value of resistor R_{11} in series with the diode connected to the contrast control pin may be chosen to give the desired reduction of contrast before a reduction of brightness is caused by beam-current limiting. (A nominal value of 1kΩ for R_{11} is shown in Fig.21.) This circuit limits the beam current of the picture tube to a maximum mean value of about 1.5mA.

Chroma signal fader circuit

As the aerial signal to the receiver falls below the threshold of the a.g.c., the luminance input signal to the decoder also falls. However, the decoder a.c.c. will maintain the chroma signal voltage beyond the a.g.c. threshold, thus giving the effect of increased saturation of coloured noise, while at the same time the luminance noise remains constant. In practice, this effect, producing an apparent increase in chroma saturation, may be present for only about 3dB below the a.g.c. threshold point before colour-killing occurs.

The circuit shown in Fig.22 removes any such increase in saturation, and requires only six resistors, one diode, and one capacitor in addition to the components of the general circuit of the decoder shown in Fig.3. The circuit adds a negative-going voltage, derived by peak detection of the colour burst, to the a.c.c. voltage at pin 3 of the TDA2560 integrated circuit IC_1. The diode D_1 is biased to about 4V and is made to conduct during the burst period by the sandcastle pulse applied through R_3, R_2, and C_2. The negative-going voltage from this peak detector has no effect on the a.c.c. voltage at pin 3 of the TDA2560 integrated circuit, provided that IC_2 is operating over its linear range and not limiting, as indicated by the output voltage at pin 13. This output voltage has a maximum value of about 5.5V, and on reaching this value can no longer counteract the effects of the peak-detected a.c.c. voltage. As a result of the use of the peak detector, therefore, excessive signal noise causes a reduction of the a.c.c. gain and saturation, until the point at which colour-killing occurs is reached.

Delay circuit for the black-level clamp pulse

The upper part of the sandcastle waveform is used to gate the black-level clamp for the luminance signal in the TDA2650 integrated circuit. The nominal phase of the upper part of the sandcastle waveform is such that it overlaps the line sync pulse (as provided by the TDA2590 integrated circuit) by about 0.5μs. The d.c. level of the luminance signal depends on the extent of this overlap and, therefore, variations in the phase influence the black-level of the picture. However, this influence is only

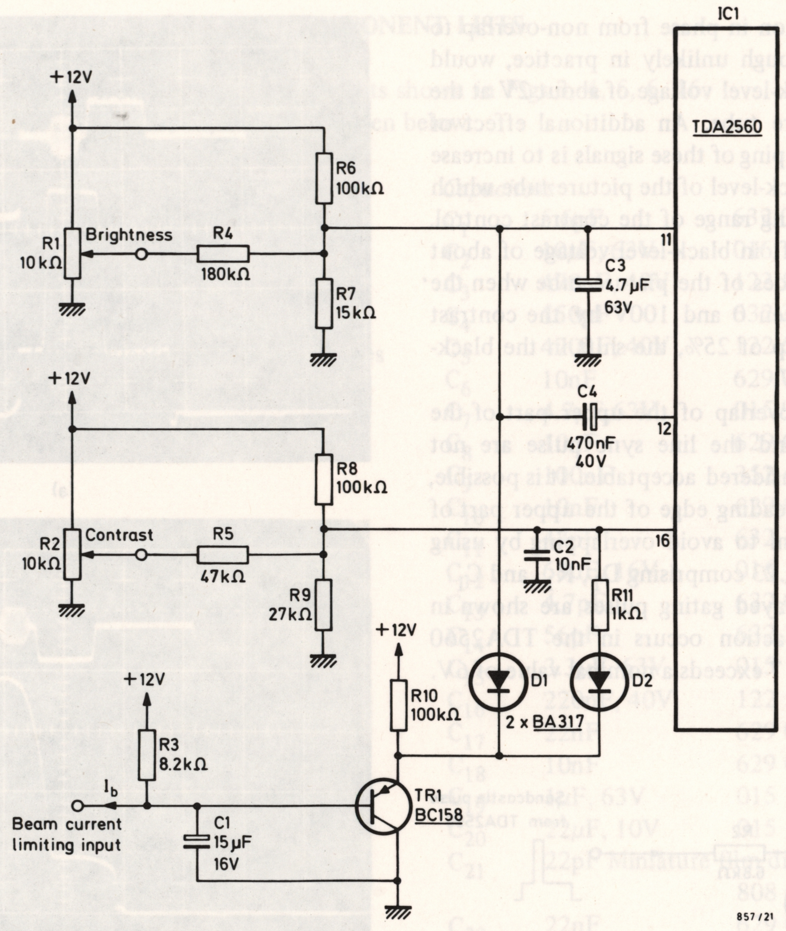

Fig.21 – Beam-current limiting circuit applied to brightness and contrast controls

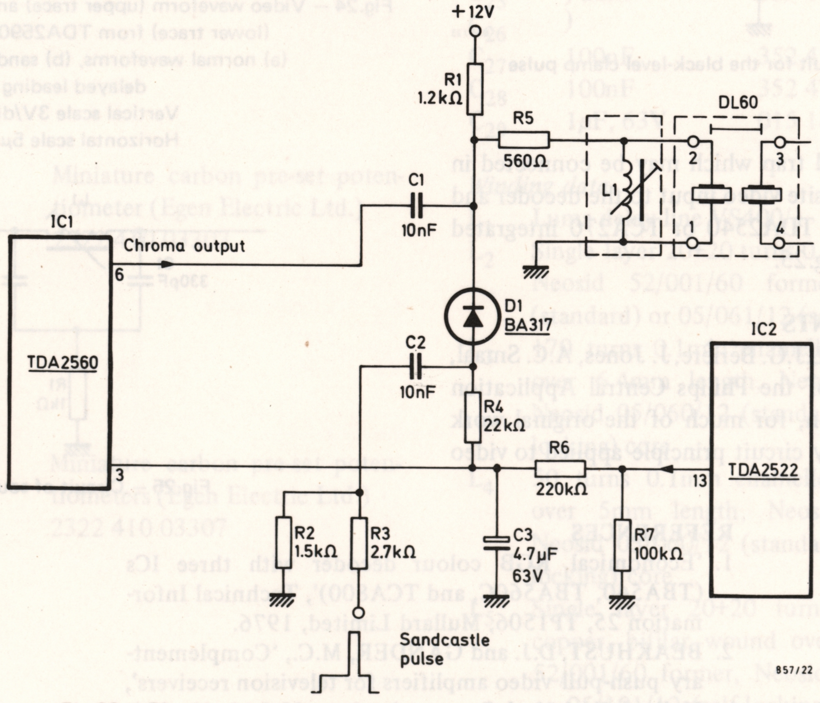

Fig.22 – Chroma peak-detector circuit interfaced with the general circuit of the RGB decoder shown in Fig.3

slight, because a variation in phase from non-overlap to complete overlap, although unlikely in practice, would result in a shift in black-level voltage of about 2V at the cathodes of the picture tube. An additional effect of variations in the overlapping of these signals is to increase the variation in the black-level of the picture tube which occurs over the operating range of the contrast control. With no overlap, a shift in black-level voltage of about 1V occurs at the cathodes of the picture tube when the drive is adjusted between 0 and 100V by the contrast control. With an overlap of 25%, the shift in the black-level voltage is about 5V.

The effects of the overlap of the upper part of the sandcastle waveform and the line sync pulse are not serious and may be considered acceptable. It is possible, however, to delay the leading edge of the upper part of the sandcastle waveform to avoid overlapping by using the circuit shown in Fig.23 comprising D_1, R_1, and C_1.

The normal and delayed gating pulses are shown in Fig.24; the clamping action occurs in the TDA2560 when the voltage at pin 7 exceeds a nominal value of 6V.

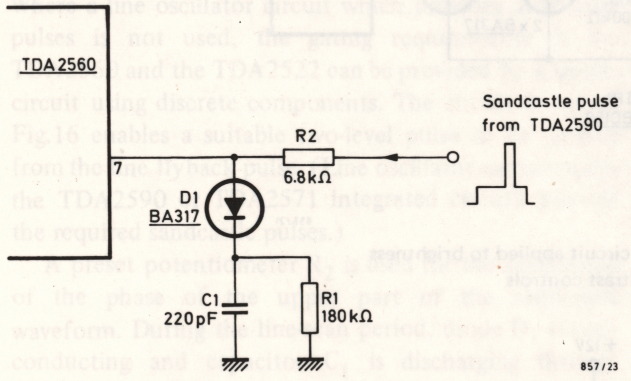

Fig.23 – Delay circuit for the black-level clamp pulse

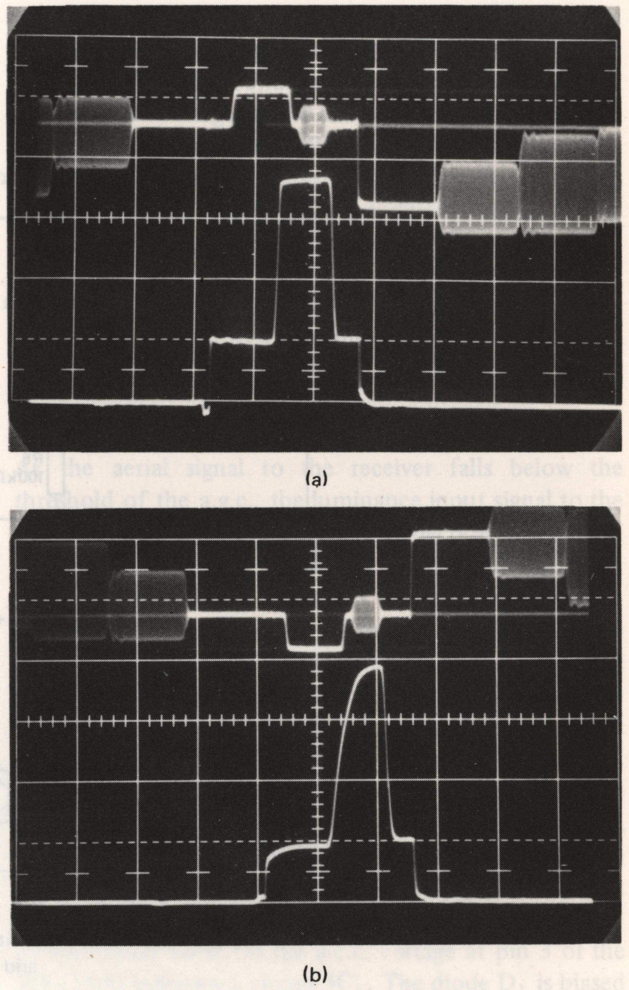

Fig.24 – Video waveform (upper trace) and sandcastle waveform (lower trace) from TDA2590 integrated circuit: (a) normal waveforms, (b) sandcastle waveform with delayed leading edge.
Vertical scale 3V/division
Horizontal scale 5μs/division

Sound trap

The circuit of a sound trap which may be connected in series with the composite video input to the decoder and the output from the TDA2540 or TCA270 integrated circuits is shown in Fig.25.

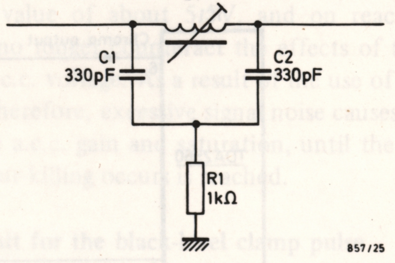

Fig.25 – Circuit of sound trap

ACKNOWLEDGEMENTS

Recognition is due to L.J.G. Bérière, J. Jones, A.C. Smaal, and D.J.A. Teuling of the Philips Central Application Laboratory, Eindhoven, for much of the original work on the complementary circuit principle applied to video amplifiers.

REFERENCES

1. 'Economical RGB colour decoder with three ICs (TBA540, TBA560C, and TCA800)', Technical Information 25, TP1506, Mullard Limited, 1976.
2. BEAKHUST, D.J. and GANDER, M.C., 'Complementary push-pull video amplifiers for television receivers', **Mullard Technical Communications**, Vol.13, No.128, October 1975, pp.294 to 301. Available as reprint TP1539.

COMPONENT LISTS

Details of the components shown in Figs.3, 4, 5, 6, 16, 21, 22, 23, and 25 are given below.

RGB decoder circuit (Fig.3)

Resistors

All resistors CR25 5% unless otherwise stated

R_1	10kΩ)	Linear carbon potentiometers (Egen Electric Ltd.) CP23 series
R_2	10kΩ)	
R_3	47kΩ)	
R_4	68kΩ	
R_5	180kΩ	
R_6	56kΩ	
R_7	1.2kΩ	
R_8	100kΩ	
R_9	22kΩ	
R_{10}	100kΩ	
R_{11}	15kΩ	
R_{12}	82kΩ	
R_{13}	5.6kΩ	
R_{14}	1.8kΩ	
R_{15}	5.6kΩ, 2% MR25	
R_{16}	3.9kΩ	
R_{17}	680Ω	
R_{18}	4.7kΩ	
R_{19}	10kΩ, 2% MR25	
R_{20}	27kΩ	
R_{21}	10kΩ	
R_{22}	1.8kΩ	
R_{23}	560Ω	
R_{24}	1kΩ	
R_{25}	6.8kΩ	
R_{26}	1.5kΩ	
R_{27}	100Ω	
R_{28}	6.8kΩ	
R_{29}	470Ω	Miniature carbon pre-set potentiometer (Egen Electric Ltd.) 2322 410 03303
R_{30}	6.8kΩ	
R_{31}	750Ω	
R_{32}	1.2kΩ	
R_{33}	220Ω	
R_{34}	8.2kΩ	
R_{35}	82kΩ	
R_{36}	)	Miniature carbon pre-set potentiometers (Egen Electric Ltd.) 2322 410 03307
R_{37}	) 10kΩ	
R_{38}	)	
R_{39}	8.2kΩ	
R_{40}	10kΩ	

Diodes

D_1	BZX79-C10 to C15 (not critical)
D_2	BZX79-C7V5

Capacitors

C_1	5.6pF	632 09568
C_2	10μF, 63V	016 18109
C_3	470nF, 40V	122 57477
C_4	150pF	632 34151
C_5	470nF, 40V	122 57477
C_6	10nF	629 02103
C_7	4.7μF,63V	015 90003
C_8	10nF	629 02103
C_9	100nF	352 47104
C_{10}	10nF	629 06103
C_{11}	47pF	632 34479
C_{12}	68μF, 16V	016 15689
C_{13}	4.7pF	632 09478
C_{14}	56pF	632 34569
C_{15}	3.3μF, 63V	015 18338
C_{16}	220nF, 40V	122 57227
C_{17}	22nF	629 02223
C_{18}	10nF	629 06103
C_{19}	1μF, 63V	015 18108
C_{20}	22μF, 10V	015 14229
C_{21}	22pF Miniature film dielectric trimmer	808 00006
C_{22}	22nF	629 02223
C_{23}	47μF, 40V	016 17479
C_{24}	)	
C_{25}	) 22nF	629 02223
C_{26}	)	
C_{27}	100nF	352 47104
C_{28}	100nF	352 47104
C_{29}	1μF, 63V	015 18108

Winding data

L_1	Luma delay line VS400/1
L_2	Single layer 20+20 turns 0.1mm enamelled copper, Neosid 52/001/60 former, Neosid 05/060/12 (standard) or 05/061/12 (self-locking) core
L_3	170 turns 0.1mm enamelled copper, wavewound over 6.4mm length, Neosid 52/001/60 former, Neosid 05/060/12 (standard) or 05/061/12 (self-locking) core
L_4	50 turns 0.1mm enamelled copper, wavewound over 5mm length, Neosid 52/001/60 former, Neosid 05/060/12 (standard) or 05/061/12 (self-locking) core
L_5	Single layer 20+20 turns 0.125mm enamelled copper, bifilar wound over 6mm length, Neosid 52/001/60 former, Neosid 05/100/12 (standard) or 05/101/12 (self-locking) core. The core of L_5 should initially be adjusted to give an inductance value of 10μH for the overall winding

Integrated circuits

IC_1	TDA2560
IC_2	TDA2522
IC_3	TDA2530
IC_4	78M12CU

Crystal

8.867238MHz	4322 143 03120

PAL delay line

DL60

Class A video output stage (Fig.4)

Resistors

All resistors CR25 5% unless otherwise stated

R_1	1.8kΩ	
R_2	1.2kΩ	
R_3	68kΩ, 2% MR30	
R_4	6.8kΩ	
R_5	10kΩ	Miniature carbon pre-set potentiometer (Egen Electric Ltd.) 2322 410 03307
R_6	5.6kΩ, 10% 7W	
R_7	1.5kΩ	

Capacitor

C_1	10nF	629 06103

Diode

D_1	BZX79-C7V5

Transistor

TR_1	BF337

Class AB complementary push-pull video output stage (Fig.5)

Resistors

All resistors CR25 5% unless otherwise stated

R_1	5.6kΩ	
R_2	220kΩ	
R_3	470Ω	
R_4	1kΩ	
R_5	1kΩ	
R_6	33Ω	
R_7	33Ω	
R_8	47kΩ, 5% CR37	
R_9	1.8kΩ	
R_{10}	1.2kΩ	
R_{11}	68kΩ, 2% MR30	
R_{12}	10kΩ	
R_{13}	10kΩ	Miniature carbon pre-set potentiometer (Egen Electric Ltd.) 2322 410 03307

Capacitors

C_1	4.7nF	347 51472
C_2	2.2µF, 25V	122 56228
C_3	220nF, 40V	122 57227

Diodes

D_1	BZX79-C7V5
D_2	BAV21

Transistors

TR_1	BF423
TR_2	BF422

Class B complementary push-pull video output stage (Fig.6)

Resistors

All resistors CR25 5% unless otherwise stated

R_1	68kΩ	
R_2	1kΩ	
R_3	1kΩ	
R_4	2.2kΩ, 1W	
R_5	68kΩ	
R_6	1.8kΩ	
R_7	1.2kΩ	
R_8	68kΩ, 2% MR30	
R_9	10kΩ	
R_{10}	12kΩ	
R_{11}	10kΩ	Miniature carbon pre-set potentiometer (Egen Electric Ltd.) 2322 410 03307

Capacitors

C_1	10nF	629 06103
C_2	4.7nF	347 51472
C_3	100nF	352 47104
C_4	2.5µF, 250V	
C_5	10nF	629 06103
C_6	10nF	352 57103

Diodes

D_1	BA316
D_2	BA316
D_3	BZX79-C7V5
D_4	BAV21
D_5	BAV21

Transistors

TR_1	BF423
TR_2	BF422

Sandcastle pulse generator circuit (Fig.16)

Resistors

All resistors CR25 5% unless otherwise stated

R_1	27kΩ	
R_2	10kΩ	Miniature carbon pre-set potentiometer (Egen Electric Ltd.) 2322 410 03307
R_3	6.8kΩ	
R_4	18kΩ	

Capacitor

C_1	2.7nF	630 02272

Diodes

D_1	BA317
D_2	BA317

Beam-current limiting circuit (Fig.21)

Resistors

All resistors CR25 5% unless otherwise stated

R_1	10kΩ (R_2 in Fig.3)	
R_2	10kΩ	Linear carbon potentiometer (Egen Electric Ltd.) CP23 series
R_3	8.2kΩ	
R_4	180kΩ (R_5 in Fig.3)	
R_5	47kΩ	
R_6	100kΩ (R_{10} in Fig.3)	
R_7	15kΩ (R_{11} in Fig.3)	
R_8	100kΩ	
R_9	27kΩ	
R_{10}	100kΩ	
R_{11}	1kΩ	

Capacitors

C_1	15µF, 16V	015 15159
C_2	10nF (C_8 in Fig.3)	
C_3	4.7µF, 63V (C_7 in Fig.3)	
C_4	470nF, 40V (C_5 in Fig.3)	

Diodes

D_1	BA317
D_2	BA317

Transistor

TR_1	BC158

Chroma peak-detector circuit (Fig.22)

Resistors

All resistors CR25 5%

R_1	1.2kΩ
R_2	1.5kΩ
R_3	2.7kΩ
R_4	22kΩ
R_5	560Ω (R_{23} in Fig.3)
R_6	220kΩ
R_7	100kΩ

Capacitors

C_1	10nF (C_{10} in Fig.3)	
C_2	10nF	629 06103
C_3	4.7µF, 63V	015 90003

Diode

D_1	BA317

Delay circuit for the black-level clamp pulse (Fig.23)

Resistors

Both resistors CR25 5%

R_1	180kΩ
R_2	6.8kΩ (R_{25} in Fig.3)

Capacitor

C_1	220pF	632 58221

Diode

D_1	BA317

Sound trap circuit (Fig.25)

Resistor

R_1	1kΩ, CR25 5%

Capacitors

C_1	330pF	632 58331
C_2	330pF	632 58331

Winding data

L_1	Single layer 30 turns 0.1mm enamelled copper, Neosid 52/001/60 former, Neosid 05/060/12 (standard) or 05/061/12 (self-locking) core

Acoustic surface-wave bandpass filters

D.W. **Parker**, B.A., R.G. **Pratt**, B.Sc., F.W. **Smith**, B.Sc., and R. **Stevens**, B.Sc.
Mullard Research Laboratories

Acoustic surface waves on a substrate of piezoelectric material can be employed in an analogue bandpass filter. The frequency response of the filter is determined by the form and dimensions of the interdigital electrodes in the transmitting and receiving transducers. A relatively simple model provides a means of designing these filters in a systematic way. However, this model requires correction for factors such as diffraction, reflection, and interactions between the acoustic sources. Computer programs have been developed that design a layout for a mask-making system, with the specifications for amplitude and group-delay characteristics as the input data. The article considers, as an application, an analogue bandpass filter for use as an i.f. filter in television receivers. The devices have been developed to a point at which they can be considered for commercial production in quantity. Good results have also been obtained with the application of surface-wave techniques to Gaussian filters, matched filters and wideband filters.

INTRODUCTION

It is only ten years since the invention of the interdigital transducer made the use of acoustic surface waves a practical possibility in systems for signal processing. Since that time many laboratories have been working on a wide range of circuit elements based on acoustic surface waves. At Mullard Research Laboratories a group of scientists have devised computer methods for designing filters that have a specified frequency response. One of the devices that have been developed with the aid of these methods is an analogue bandpass filter suitable for use as an intermediate-frequency filter in television receivers.

Technical background

The interdigital transducer, two comb-like electrodes interlocking with one another, allows electrical signals to be efficiently and linearly converted into acoustic signals in piezoelectric material; the acoustic signals propagate in the form of surface waves.

If two such transducers are applied to a piezoelectric substrate, the acoustic surface waves generated by the first transducer can be reconstituted to an electrical signal in the second transducer, giving a filter, as we shall explain in more detail later. The frequency characteristic of the filter depends on the geometry of the two transducers (Ref.1).

The designation 'acoustic' is perhaps a little misleading, since it might suggest that the surface waves had frequencies in the audio range (about 20 to 18 000Hz). In fact acoustic surface waves can have very high frequencies (up to several GHz); the feature they have in common with sound waves is that the signals propagate via oscillations of particles in the material. The velocity of propagation of the surface waves is a few km/s, and the wavelength varies from about 1mm at 3MHz to 1μm at 3GHz. From the values quoted for the wavelength it can be seen that the dimensions of acoustic surface-wave filters will be of the order of millimetres; they are therefore about 10^5 times as small as their electromagnetic counterparts.

The nature of the acoustic surface-wave filter is such that the initial design costs are relatively high but large numbers of the devices can be produced cheaply. Like integrated circuits – but to a lesser degree – these filters are consequently mainly suitable for mass production.

Our work has been chiefly directed towards the design and manufacture of acoustic surface-wave filters that can be used as i.f. filters in television receivers. Not only are these components that are required in large numbers, but in addition surface waves turn out to be extremely convenient for use in this particular frequency range.

In this article we shall describe how techniques have been developed to design and make such filters and how problems encountered have been solved. Examples of filters we have made, suitable for use in two different television systems, will be given. In addition, we shall describe filters designed for other applications. First of all, however, we shall look more closely at the details of the operation of surface-wave filters and at the relationship between the electrode geometry and the frequency characteristic.

CONSTRUCTION AND OPERATION OF A SURFACE-WAVE FILTER

Fig.1 is a schematic diagram showing the general appearance of a surface-wave filter. The easiest way of understanding its operation is to consider each finger of the two electrodes as a linear source of surface waves, located at the centre-line of that finger. The strength of such an acoustic source in the input transducer depends on the length l by which the fingers overlap; the source strength is to a first approximation directly proportional to this 'finger-length', which can have different values from finger to finger. The acoustic signal that travels over the surface of the substrate therefore consists of components that can be considered as delayed acoustical replicas – of differing strengths – of the electrical input signal, a situation that is characteristic of the 'transversal' filter. At a given place on the surface of the substrate these components will be in phase at certain frequencies and will add to form a strong signal. At other frequencies they will be out of phase and will cancel or almost cancel.

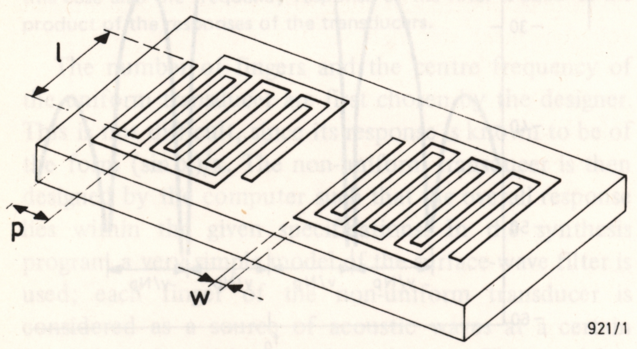

Fig.1 – Simplified representation of a surface-wave filter. On a piezoelectric substrate there are two transducers, each consisting of two comb-shaped electrodes whose fingers enmesh with one another ('interdigital electrodes'). One of the transducers generates surface waves, the other converts them into an electrical signal. In the case shown the distance l, over which the fingers overlap one another, is the same for all fingers ('uniform transducer'). In general this is not the case. In the filters that are discussed in this article the width w of the fingers is usually a quarter of their spacing p.

It can be shown that the frequency response F(ω) of a transducer consisting of a number of equidistant line sources, as in the simple model described above, can be described by a Fourier series whose coefficients are given by the strengths of the acoustic sources. This implies that the frequency response is a periodic function of the frequency. The period Ω of this function is equal to twice the centre frequency ω_0 of the first transmission band; see Fig.2. The passbands are identical and they are symmetrical about their centre frequencies. If all the fingers are of the same length and width – i.e. it is a 'uniform' transducer – the first passband is of the form (sin x)/x, where x is given by:

$$x = \frac{(\omega - \omega_0)Np}{2v}.$$

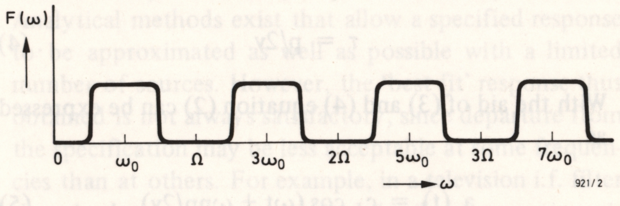

Fig.2 – The frequency response of a hypothetical transducer, consisting of a number of equidistant line sources (spacing ½p), is a periodic function. The period Ω is equal to $2\pi v/p$; v is the propagation velocity of the surface waves. The passbands at ω_0, $3\omega_0$, $5\omega_0$ etc. are all symmetrical in this case and are similar. In a practical transducer, however, the passbands are *not* all similar, because of the effects of the finger width. For example, in transducers for which w = ¼p, the band at $3\omega_0$ is missing.

Here N is the number of pairs of fingers and v is the phase velocity of the surface wave. At the centre frequency ω_0 the wavelength of the surface wave is equal to the period p of the interdigital electrodes.

Since in reality the fingers are not true line sources, the real frequency responses differ from the one shown in Fig.2: their heights are markedly different and some are virtually absent. For transducers in which w = ¼p, this is for example the case for the passband at $3\omega_0$. Since in practice the higher passbands will usually be situated outside the band passed by the system including the filter, we can confine our attention to the passband around ω_0. The effect of the finger-width on the shape of the first passband is relatively small.

If we assume that the electrical input signal e(t) is sinusoidal and of the form

$$e(t) = \cos \omega t, \qquad \ldots(1)$$

This article appeared in **Philips Technical Review**, Vol.36, No.2, 1976, pp.29 to 43.

then the n^{th} component of the acoustic signal is given by

$$a_n(t) = c_n \cos(\omega t + \phi_n), \qquad \ldots (2)$$

where c_n is the strength of the corresponding source and ϕ_n represents the phase shift introduced when the component $a_n(t)$ is delayed by a time τ_n with respect to e(t):

$$\phi_n = \omega \tau_n. \qquad \ldots (3)$$

Since we are considering line sources regularly spaced at a distance of ½p, the delay times of the acoustic-signal components are multiples of the time τ in which the waves travel a distance ½p:

$$\tau = p/2v. \qquad \ldots (4)$$

With the aid of (3) and (4) equation (2) can be expressed as

$$a_n(t) = c_n \cos(\omega t + \omega np/2v). \qquad \ldots (5)$$

The acoustic signal s(t) is then given by

$$s(t) = \sum_n c_n \cos(\omega t + \omega np/2v). \qquad \ldots (6)$$

A linear system that responds to an input $e(t) = \cos \omega t$ with an output given by (5) can be described by the frequency response $c_n e^{-j\omega np/2v}$. From this we can conclude that the input transducer, which responds to an input signal $e(t) = \cos \omega t$ with an acoustic signal given by (6), has a frequency response given by

$$F(\omega) = \sum_n c_n e^{-j\omega np/2v}. \qquad \ldots (7)$$

From (7) it follows that $F(\omega)$ is periodic with a period Ω equal to $4\pi v/p$. The expression (7) can be considered as a Fourier series expansion of the periodic function $F(\omega)$. For a certain specified frequency response, the strengths c_n of the acoustic sources can be found from the equation

$$c_n = \frac{1}{\Omega} \int_{-\Omega/2}^{\Omega/2} F(\omega) e^{j\omega np/2v}. \qquad \ldots (8)$$

Since the nature of the surface-wave filter requires the sum of all the source strengths to be zero,

$$\sum_n c_n = 0,$$

d.c. transmission is not possible, and this excludes the lowpass filter from the applications of surface-wave filters.

Similar reasoning applies for the receiving transducer. The sensitivity of the pairs of fingers functioning as receivers – like the strength of the acoustic sources – is approximately proportional to the length l. In the case of a uniform receiving transducer with the same number of fingers as the transmitting transducer, the overall filter response is of the form $\{(\sin x)/x\}^2$. The bandwidth of this filter, measured between the two central nulls, will be 2v/Np; the other nulls will be separated by v/Np, as shown in Fig.3.

In the general case in which neither transducer is uniform, the frequency response of the filter is not the same as the product of the frequency responses of the two individual transducers. This is the case, however, if only one of the transducers is non-uniform. It is therefore in general desirable to try to obtain a particular filter response with one uniform and one non-uniform transducer.

Of course, the simple model that we have used here to explain the operation of the filter has to be corrected for such things as diffraction of the acoustic waves and the fact that the sources are not independent of each other. Nevertheless, it provides a means of designing these filters in a systematic way. All that needs to be done to obtain a particular frequency response, in principle, is to find the Fourier series of a periodic repetition of that response. This gives a list of the strengths of the sources required and of their positions. In the following section we shall explain how these procedures are put into practice. We shall also explain how an asymmetrical characteristic can be obtained.

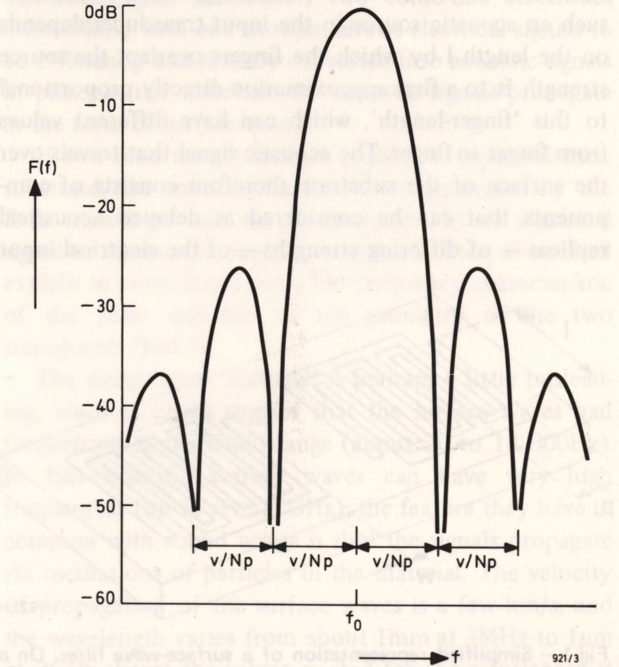

Fig.3 – Amplitude response of a surface-wave filter with uniform transducers. In this case the response is the product of the responses of the input and output transducers. Since both have the form (sin x)/x, the amplitude response has a shape that can be described by the function $\{(\sin x)/x\}^2$. The bandwidth of the filter, measured between the first two zero points from the centre, is 2v/Np, and the rest of the zeros (points with infinite attenuation) have a spacing of v/Np; N is the number of pairs of fingers.

DESIGNING SURFACE-WAVE FILTERS

Our technique for surface-wave filter design uses a set of computer programs that require very little intervention by the user. A specification of relative amplitude and group delay as a function of frequency (with tolerances) is given, and the computer programs design the filter as far as the point at which layout data can be produced for a standard automatic mask-making system.

The principal method that we have used for variation of the source strength, and hence to obtain the desired frequency response, is to vary the length l by which the fingers overlap; the width w is kept constant. In all the filters we have made, we varied the length of the fingers in only one of the transducers (Fig.4): in that case the total frequency response of the filter is the product of the individual responses.

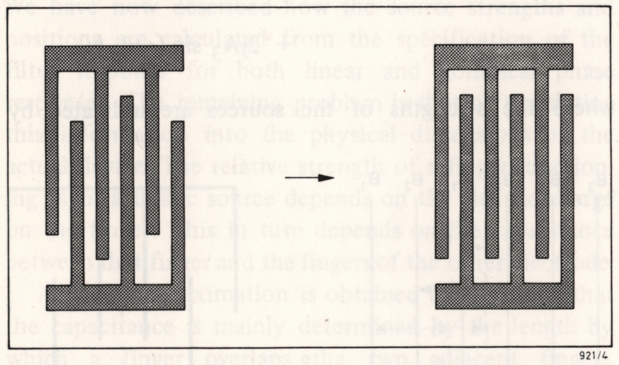

Fig.4 – Surface-wave filter with a single uniform transducer (the receiver) and another one with fingers of dissimilar length. In this case also the frequency response of the filter is equal to the product of the responses of the transducers.

The number of fingers and the centre frequency of the uniform transducer are first chosen by the designer. This is not difficult, since its response is known to be of the form (sin x)/x. The non-uniform transducer is then designed by the computer such that the overall response lies within the given specifications. In the synthesis program a very simple model of the surface-wave filter is used; each finger of the non-uniform transducer is considered as a source of acoustic waves at a certain strength and position on the substrate. This model is usually adequate for most filters of reasonably wide 'aperture' (i.e. the length of the longest finger of the electrodes) and not too great a bandwidth. Other programs are also available for checking whether second-order effects, such as diffraction, reflection, interaction between sources, etc., will significantly alter the response of the filter.

The first step in the design is to calculate a target response for the non-uniform transducer, together with the permitted tolerances. When this response is repeated periodically, a Fourier series can be found that describes the response sufficiently accurately. This series then indicates the acoustic source strengths required from sources spaced regularly at half a wavelength ($\lambda_0/2$) at the centre frequency ω_0.

Two problems may now arise. In the first place the Fourier series gives in general an infinite number of terms, and hence sources. Secondly, if an amplitude response is required that is asymmetrical about ω_0, the Fourier coefficient will be complex.

In a practical device the number of sources will not of course be infinitely large. This can perturb the response in such a way that it may depart from the specification. Analytical methods exist that allow a specified response to be approximated as well as possible with a limited number of sources. However, the 'best fit' response thus obtained is not always satisfactory, since departure from the specification may be less acceptable at some frequencies than at others. For example, in a television i.f. filter the absolute accuracy required in the trap regions is considerably greater than that in the centre of the passband, where some ripple (± ½dB) is tolerable. Our approach is to limit the number of sources to a value that we have found from experience to give a good chance of meeting the specification. The source strengths are then corrected until the response lies within the given tolerance. In our approach the response of the transducer with the limited number of fingers is compared with the specification and a number of the most serious errors are identified. These are then corrected by 'adding' to the original transducer a number of correcting transducers, one for each error point (Ref.2). Usually, new errors will then appear, so the process is repeated. In practice, it is found either that the response is brought fairly rapidly within the specification, or that the number of points with large errors rapidly increases, the second case indicates that more sources are required and that the design procedure should be started again.

The second problem arises if an asymmetrical amplitude response is required. The fact that complex Fourier coefficients are found in this case means that the sources must generate acoustic signals not only with different amplitudes, but also with different phases. This is not really practical, of course, but an approximation that is valid at one frequency is to give each source a different delay by moving their positions away from the regular $\lambda_0/2$ spacings, thus changing the relative phases. In the design procedure both the strength and position of the sources now have to be varied to bring the filter response within the specification. We have a technique for doing this, but because of the approximations good results are only obtained if the asymmetry of the amplitude response is not too great.

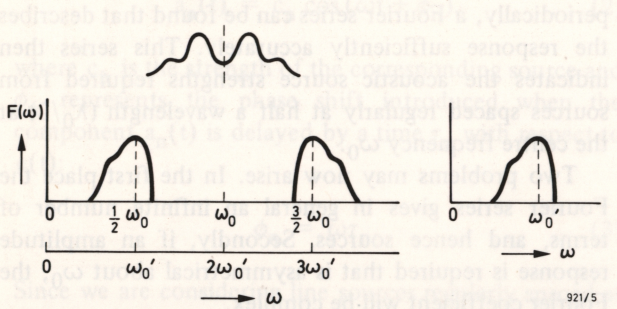

Fig.5 – Illustrating the method for making filters with an asymmetrical frequency response without making use of sources with a phase difference between them (i.e. with a complex source strength). If the distance p (see Fig.1), starting at half the wavelength corresponding to ω_0, is decreased, the central maximum of the first passband (see Figs.2 and 3) becomes lower and eventually the band splits into two parts. Because of the desired symmetry about ω_0 these two parts of the band are mirror images of one another, but each one is itself asymmetrical. If p is chosen such that the partial bands are located at $\frac{1}{2}\omega_0$ and $\frac{3}{2}\omega_0$ and the ratio of w to p in the other transducer is made such that the third harmonic is suppressed, then the filter obtained has an asymmetrical amplitude response about the frequency ω_0' (= $\frac{1}{2}\omega_0$). The finger spacing in the first transducer is then half that in a filter with a symmetrical response about ω_0'.

A way out of this problem is obtained by considering the desired asymmetrical response as the left-hand half of a symmetrical one, in the manner indicated in Fig.5. The Fourier coefficients of this new function are real, and only the problem of the finite number of sources remains (Ref.3). The transducers produced by this technique have sources spaced at a constant distance of $\lambda_0/4$, and are called double-finger transducers (Ref.4). A disadvantage of the small electrode spacing is that the resolution of the fabrication process must be twice as large.

The phase response

So far we have not considered the phase response of the filter. When the acoustic sources in the transducer are symmetrically arranged about the centre-line of the transducer, the phase response will be linear, irrespective of the amplitude response. The design procedures described above all impose this restriction and therefore only produce filters with linear phase response. Sometimes, however, a prescribed nonlinear phase response is required. Such filters are chiefly used in some European countries as i.f. filters in television receivers, as we shall explain more fully later. We will now give some attention to the way in which such filters are designed.

Our method for designing a filter with a nonlinear phase response is based on the two possible ways that exist for designing a transducer with a linear phase response (see Fig.6). The symmetrical transducer (Fig.6a) has sources of equal magnitude and sign on either side of the centre-line. Using the Fourier series expansion to describe the frequency response of the symmetrical transducer, we find:

$$F_s(\omega) = B_3 e^{j\omega d_3/v} + B_2 e^{j\omega d_2/v} + B_1 e^{j\omega d_1/v} + $$

$$+ B_1 e^{-j\omega d_1/v} + B_2 e^{-j\omega d_3/v} + B_3 e^{-j\omega d_2/v}$$

$$= 2B_1 \cos(\omega d_1/v) + 2B_2 \cos(\omega d_2/v) +$$

$$+ 2B_3 \cos(\omega d_3/v),$$

where the strengths of the sources are indicated by $B_{1,2,3}$ and the distances from the centre-line to the source by $d_{1,2,3}$. For the frequency response of the asymmetrical transducer (Fig.6b) we find:

$$F_a(\omega) = A_3 e^{j\omega d_3/v} + A_2 e^{j\omega d_2/v} + A_1 e^{j\omega d_1/v} -$$

$$- A_1 e^{-j\omega d_1/v} - A_2 e^{-j\omega d_2/v} - A_3 e^{-j\omega d_3/v}$$

$$= 2jA_1 \sin(\omega d_1/v) + 2jA_2 \sin(\omega d_2/v)$$

$$+ 2jA_3 \sin(\omega d_3/v),$$

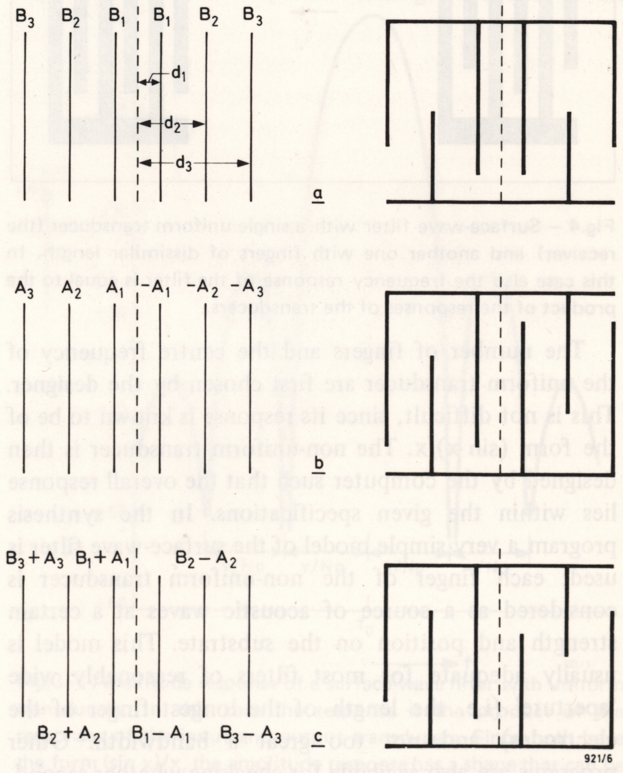

Fig.6 – The diagrams on the right show schematic representations of (a) a transducer with even symmetry, (b) a transducer with odd symmetry and, (c) an asymmetrical transducer, formed by combining an odd and an even transducer. The source strengths are indicated by $A_{1,2,3}$ and $B_{1,2,3}$, the positions of the fingers by $d_{1,2,3}$.

where the strengths of the sources are indicated by $A_{1,2,3}$ and the polarity by a plus or a minus sign. From both expressions we conclude that the symmetrical transducer has a real frequency response, representing a zero phase shift for all frequencies, while the asymmetrical transducer has an imaginary frequency response (note the factor j), representing a 90° phase shift at all frequencies.

The method used for designing a nonlinear phase filter is as follows. The required phase and amplitude responses are resolved into two components, each with a linear phase response but with a phase difference of 90° with respect to each other. Each of the components can be realised with a single transducer: one with a symmetrical transducer, the other with an asymmetrical transducer. If the source positions are arranged to be the same in both transducers, they can be combined to produce a single transducer, which will have a nonlinear phase response. The combination is done by adding the strengths of corresponding sources, as shown in Fig.6c.

Calculation of the electrode configuration

We have now described how the source strengths and positions are calculated from the specification of the filter response for both linear and nonlinear phase responses. The remaining problem is that of translating this information into the physical dimensions of the actual device. The relative strength of a finger functioning as an acoustic source depends on the electric charge on the finger. This in turn depends on the capacitance between that finger and the fingers of the other electrode.

A good approximation is obtained by assuming that the capacitance is mainly determined by the length by which a finger overlaps the two adjacent fingers. Allowance does however have to be made for some end effects. For example, at the end of a finger a small additional amount of charge is present due to fringing fields to neighbouring electrodes. In addition, the capacitance per unit length at the end of the interdigital array is not the same as at the centre, at least for a long array. All these effects are allowed for in a program that calculates the length of each finger from a list of the required sources.

A particular set of source strengths can only be obtained with a single configuration, and it may be that this structure is 'skewed', as shown in Fig.7. This will occur, for example, when the fingers of one of the two electrodes have a relatively short overlapping length with the adjacent finger to the left and a relatively long overlapping length with the finger to the right. A skewed transducer has an unnecessarily large aperture, and hence an increased insertion loss. Such an undesirable configuration can be avoided by synthesising a set of sources that not only meets the specified frequency response, but also satisfies some special rules for preventing skewing. This method has been found to work in practice and is included in our filter-synthesis program.

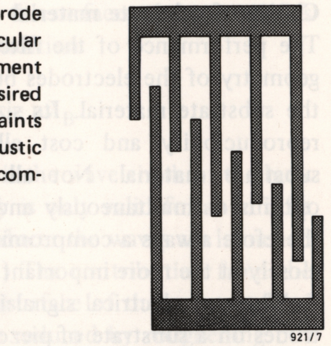

Fig.7 – In seeking an electrode design that will give a particular response, a 'skewed' arrangement may be indicated. This undesired result can be avoided if constraints on the strength of the acoustic sources are included in the computer program.

FILTER MANUFACTURE

The end result of the design process described in the preceding section is a punched tape suitable for the control of an automatic cutting machine. This produces a mask (the artwork) for the photolithographic process. From there on the electrodes are formed in a sputtered or evaporated metal layer (usually gold or aluminium) on the surface of the substrate by standard processes well known to manufacturers of integrated circuits. Since only one mask is required there are no problems of alignment*.

However, other problems occur, which are peculiar to surface-wave devices. The electrode systems are large by integrated-circuit standards (of the order of millimetres), and the fingers can be long and thin. Fabrication problems impose a lower limit on the spacing of the fingers, which determines the highest frequency the filter can handle. For conventional ultraviolet photolithography of double-finger transducers on a $Bi_{12}SiO_{20}$ substrate, for example, this highest frequency is about 250MHz. If an electron beam is used instead of light, this limit can be raised to about 1GHz. Since the transducers are so large, it is important to ensure that the optical system does not distort the finger shapes as this would degrade the performance of the filter.

The propagation surface of the substrate must be carefully polished to remove scratches and imperfections introduced when it was cut. There are two reasons for this. Firstly, surface scratches may cause breaks in individual fingers, which would affect the frequency response. Secondly, since the energy of the surface wave is concentrated within a layer one or two wavelengths deep, its propagation may be affected by damage to that layer. As an example, the surface wavelength at a frequency of 37MHz on a (100) plane of $Bi_{12}SiO_{20}$ with propagation in the ⟨110⟩ direction is only 45μm. At 370MHz it is about 4.5μm, and so on.

Once the filter has been made, it must be packaged, to protect the substrate from dirt and moisture, which would cause damping of the surface waves. The packaging must not of course interfere with the propagation surface.

---

*Important contributions to the method of applying the electrodes were made by A.L. Karr of these laboratories.

Choice of substrate material

The performance of the filter depends not only on the geometry of the electrodes but also on the properties of the substrate material. Its size, insertion loss, stability, reproducibility and cost all depend directly on the substrate material. Not all of these factors can be optimised simultaneously and the choice of materials is therefore always a compromise. We shall now look more closely at the more important material properties.

When an electrical signal is applied to a pair of electrodes on a substrate of piezoelectric material, not all of the energy is converted into acoustic waves. Some of the energy is stored in the capacitor formed by the two electrodes. The ratio of the stored to the radiated energy is determined by the square of the electromechanical coupling constant k. The insertion loss is directly dependent on the value of this constant, which means that a material with a high value of k is desirable. (The electrode capacitance can always be tuned out with an inductance, of course, but this is not always convenient and in any case will reduce the bandwidth of the filter.) In single-crystal materials – which are usually used – k is a function of the direction and plane of propagation, given by (Ref.5)

$$k^2 = \frac{2(v - v_c)}{v},$$

where v is the free surface velocity and v_c is the velocity when the surface is covered by a massless perfect conductor. Both v and v_c can readily be computed from the basic constants of the material as functions of the plane and direction of propagation. We have used the approach to calculate, for example, the variation of k in the principal planes of $Bi_{12}GeO_{20}$ and $Bi_{12}SiO_{20}$ (Refs.6 and 7).

Another important property of the material is the velocity v of the surface wave. The importance of this can best be understood if we consider a filter consisting of two uniform transducers like those shown in Fig.1; all the fingers have the same length l, width w and period p. As mentioned above, the period will be equal to the wavelength at the frequency ω_0 for which the insertion loss is a minimum. In the frequency and temperature range of interest, the velocity does *not* depend on the frequency. The positions of the maxima and the nulls (see Fig.3) will thus depend directly on the velocity, which is fortunately highly reproducible from crystal to crystal (to better than 0.1%) and does not vary with time, at least in single crystals. The velocity does however vary with temperature. (For $Bi_{12}SiO_{20}$ this, together with the temperature dependence of the dimensions, gives a temperature coefficient for the delay of about $+118 \times 10^{-6}/°C$.) It is therefore necessary to choose a material in which the temperature coefficient is low enough for the particular application. If a very high stability is required, it is possible to make use of certain planes in quartz (e.g. the ST cut), for which the first-order term of the temperature coefficient is zero; unfortunately the value of k^2 is then very low. This is all too common a situation, in which a compromise choice has to be made†.

Problems

In the model used for calculating the filter response it is assumed that each finger launches a plane wave. If the finger is short this assumption is not justified, because of diffraction effects, and corrections are necessary. However, even if the individual fingers do all launch plane waves, the beam that emerges from the transducer will not necessarily have a plane wavefront. This is related to the fact that in a transducer with unequal fingers the waves that propagate in different parts of the aperture do not always pass under the same amount of electrode metal. Since the velocity under the metal layer is less than that on the free surface (by about 1 to 2%) the wavefront will be distorted. This can be corrected by including inactive or ‘dummy’ fingers (Ref.8) in the transducer, as can be seen in Fig.8.

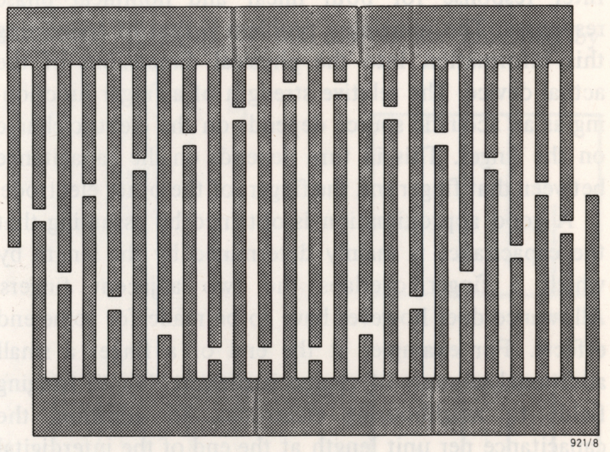

Fig.8 – Transducer with fingers of dissimilar length, which has ‘dummy’ fingers. Besides the normal active fingers inactive ones are included as well; if these fingers were not present the wavefront of the transmitted wave would not be truly planar.

Attention must also be paid to the fact that the waves are partially reflected from the fingers themselves, as a result of the change in velocity at the interface between the free surface and the part covered by the metal. Also the fingers in a transducer can detect and reradiate waves launched earlier, and this can degrade the filter performance, especially the pulse response. This effect can be minimised by using the double-finger configurations. In these designs the finger spacing is $\frac{1}{4}\lambda_0$, so that at the centre frequency the reflections from adjacent fingers are of opposite phase. If, because of fabrication problems, double-finger designs cannot be used, it is possible to use a compromise design in which the active fingers are single but the inactive ones are double (Ref.9); see Fig.9. This considerably reduces the interaction.

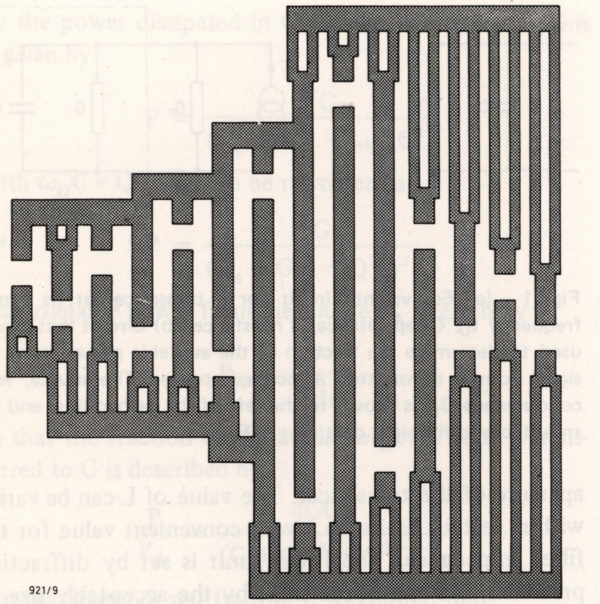

Fig.9 – Transducer with very low interaction between the acoustic sources. In this transducer the inactive fingers are doubled over part of their length, at a spacing of $\frac{1}{4}\lambda_0$, so that the reflected waves cancel.

The electrode structure used to launch the surface waves can also launch waves into the bulk of the material. These waves can cause unwanted responses at frequencies that depend on their velocity. An example of the effect of these waves on the amplitude response of the filter is shown in Fig.10. For a periodic radiating structure waves are launched at an angle θ to the surface, where θ satisfies the usual phase-matching condition:

$$p \cos\theta = n\lambda_B.$$

Here n is an integer and λ_B is the wavelength of the bulk wave. (Strictly, this equality is only valid for an infinite transducer; in a finite transducer the waves are launched over a range of values of λ.) The contribution from the waves that strike the lower surface of the substrate and are reflected from it can be reduced by roughening this surface so that they are scattered. The waves, however, that are launched at small values of θ, so that they reach the receiving transducer without being reflected from the lower surface, cannot be reduced in this way. The only solution is to choose a direction of propagation in which these waves are not too strongly excited (Ref.10).

Finally, we have to deal with the fact that in addition to the direct acoustic path from the transmitting to the receiving transducer, there are at least three other ways for an input signal to reach the receiving transducer, each with its own delay time.

The first way in which the input signal can reach the output transducer is direct electrical breakthrough due to the capacitive coupling between the two transducers. This can be reduced by putting an earthed metallic strip on the surface between the two transducers.

The second arises from the fact that the transducers are bidirectional; in Fig.1, for example, it can be seen that the input transducer will launch just as much surface-wave energy to the left as to the right. The wave going to the left will travel to the left-hand end of the substrate and will then be reflected to the output transducer. In a similar way, acoustic waves that pass under the output transducer will be reflected from the right-hand end of the substrate. Both of these waves will arrive at the output transducer with a delay different from that

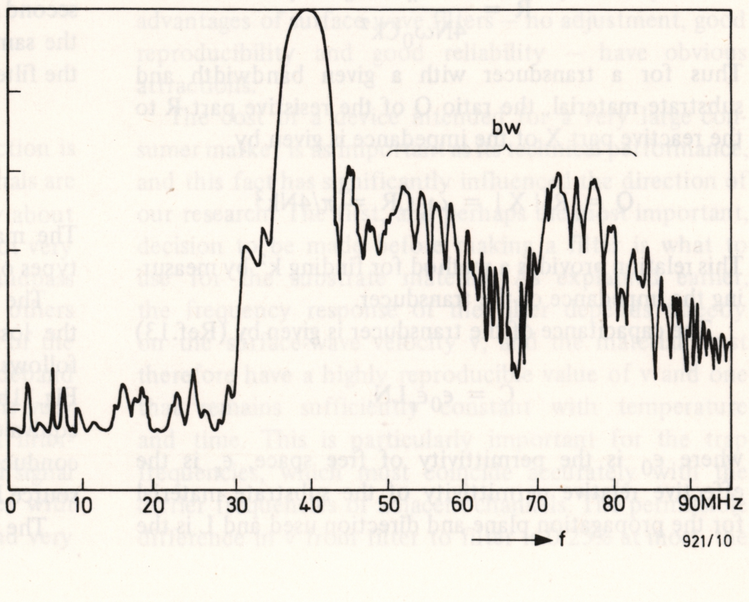

Fig.10 – Besides surface waves the transducer can also generate waves that propagate in the interior of the substrate. If these bulk waves can reach the output transducer, e.g. by a reflection from the base of the substrate, they will affect the frequency response of the filter. In the response shown this is the case in the part indicated by bw.

---

†Lithium iodate ($LiIO_3$) has been reported (V.B. Jipson, J.F. Vetelino, A. Jhunjhunwala and J.C. Field, Proc. IEEE 64, 568, 1976) as having directions in which the delay temperature coefficient is low but k^2 is high. Unfortunately, it dissolves in water and is thus not suitable for practical filters.

of the wanted signal. These end-reflected signals can usually be reduced to an acceptable level by setting the ends of the substrate at an angle and by putting absorbent material in their path.

The third way in which a delayed signal can arise is through reflection of a signal at the output transducer so that it travels back to the input transducer and is there reflected again back to the output transducer. This doubly reflected 'triple-transit' signal will have three times the delay of the wanted signal. Many methods have been devised to reduce this signal (Ref.11), but they all require a larger and more expensive substrate or an increased insertion loss, or both. The level of this triple-transit signal relative to the wanted signal depends on the k value of the substrate material: the larger k^2, the higher the level. It follows that the level of the triple-transit signal increases as the insertion loss of the filter decreases.

ACOUSTIC SURFACE-WAVE FILTERS AS CIRCUIT COMPONENTS

Apart from the frequency response, the other features of a surface-wave filter that will be of interest to a user who wishes to include it in an electrical circuit are the impedance and the insertion loss. These factors depend on the substrate material, the bandwidth, the aperture and the nature of the circuit, as will now be explained. We shall assume here that we are dealing with a filter with simple uniform transducers. In the case of non-uniform finger-lengths some modifications to the expressions will be necessary.

At the frequency of its peak response, a transducer can be represented by the simple equivalent circuit shown in Fig.11a. The power dissipated in the resistance R is a measure of the power converted into acoustic energy. It can be shown (Ref.12) that for a uniform transducer

$$R = \frac{\pi}{4N\omega_0 Ck^2}.$$

Thus for a transducer with a given bandwidth and substrate material, the ratio Q of the resistive part R to the reactive part X of the impedance is given by

$$Q = R/|X| = \omega_0 CR = \pi/4Nk^2.$$

This relation provides a method for finding k^2 by measuring the impedance of the transducer.

The capacitance of the transducer is given by (Ref.13)

$$C = \epsilon_0 \epsilon_r LN,$$

where ϵ_0 is the permittivity of free space, ϵ_r is the effective relative permittivity of the substrate material for the propagation plane and direction used and L is the aperture of the transducer. The value of L can be varied within certain limits to give a convenient value for the filter impedance. The lower limit is set by diffraction problems and the upper limit by the acceptable size of substrate.

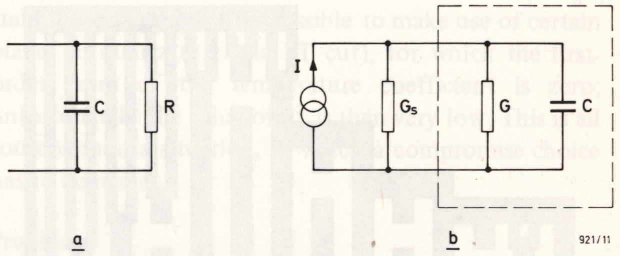

Fig.11 – (a) Equivalent circuit for a transducer at its centre frequency f_0. C capacitance, R resistance. (b) Circuit that can be used to determine the fraction of the available power from the signal source transmitted as acoustic power. The source, with conductance G_s, is shown to the left of the dashed line, and the transducer to the right of it (G = 1/R).

The insertion loss of the device is made up of two kinds of losses: those not related to matching conditions and those that are. The first category includes losses in the substrate, ohmic losses in the metallisation and losses that arise in the propagation of acoustic waves. These can usually be neglected at frequencies below a few hundred MHz for single-crystal materials at room temperature. This first category also includes the losses that arise because the transducers emit acoustic waves in two directions. In a filter with two transducers this bi-directional loss is 6dB, because each of the interdigital transducers propagates surface waves in two directions with equal power whereas in our filter we only make use of one of these directions.

If the filter is terminated by a resistance there will be a mismatch, since not all the available power from the source can be transferred to the resistive part of the transducer impedance. This introduces a loss of the second category. If both transducers of the filter have the same Q, the minimum value of the mismatch loss for the filter is given by

$$20 \log_{10} \left\{ \frac{2}{1 + \sqrt{(1+Q^2)}} \right\} \text{dB}.$$

The magnitude of the losses that will arise with other types of termination can also be calculated easily.

The expression just given for the minimum value of the loss with a resistive termination can be derived as follows. We consider the simplified circuit shown in Fig.11b. The interdigital transducer is represented by its equivalent circuit of a capacitance C in parallel with a conductance G. Power is supplied by a constant-current source I of internal conductance G_s.

The power converted into surface waves is represented by the power dissipated in G. At the frequency ω_0 this is given by

$$P = \frac{I^2 G}{(G_s + G)^2 + \omega_0{}^2 C^2}.$$

With $\omega_0 C = QG$ this can be rewritten as:

$$P = \frac{I^2 G}{(G_s + G)^2 + Q^2 G^2}.$$

The available power from the source P_A is given by

$$P_A = \frac{I^2}{4G_s},$$

so that the fraction of the available power that is transferred to G is described by

$$\frac{P}{P_A} = \frac{4GG_s}{(G + G_s)^2 + Q^2 G^2}.$$

For maximum power transfer it is required that

$$G_s = \sqrt{(G^2 + \omega_0{}^2 C^2)},$$

or

$$G_s = G\sqrt{(1 + Q^2)}.$$

It follows that

$$\left(\frac{P}{P_A}\right)_{\max} = \frac{2}{1 + \sqrt{(1+Q^2)}}.$$

This is the maximum fraction of the available power that can be transferred to G and hence is the minimum mismatch loss for a single transducer. For a filter the minimum mismatch loss is the square of this, if it is assumed that both transducers have the same value for Q.

Expressing this in decibels, we obtain the above expression.

SURFACE–WAVE FILTER FOR A TELEVISION RECEIVER

A block diagram of a television tuner and i.f. section is shown in Fig.12. The incoming u.h.f. or v.h.f. signals are converted in the tuner T into signals of frequency about 37MHz, the i.f. frequency. The tuner itself is not very selective and it is the primary function of the bandpass filter F to separate the wanted signal from any others that may be present. Since one of the sidebands of the television signal is partially suppressed (vestigial-sideband modulation), the shape of the response curve is very important for good demodulation. To prevent inter-modulation distortion in the receiver, the sound signal must be attenuated by about 20dB in the filter with respect to the peak of the filter characteristic, and very accurately located minima ('traps') must be included in the filter response to coincide with the carrier frequencies of adjacent channels. The specification for the amplitude response for a bandpass filter for the U.K. television system is shown in Fig.13.

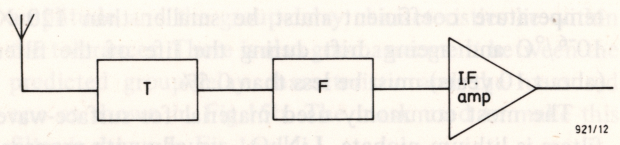

Fig.12 – In a television receiver the intermediate-frequency filter (F) is connected between the tuner (T) and the i.f. amplifier (IF amp).

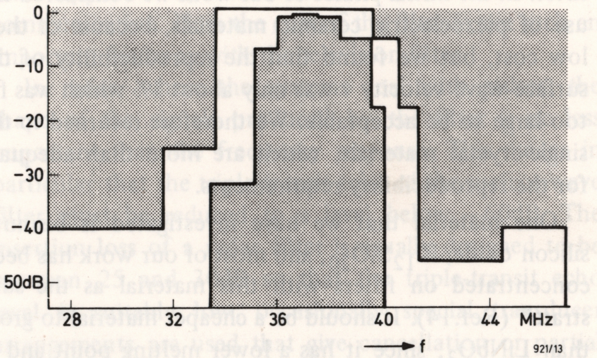

Fig.13 – Tolerance mask for the amplitude response of a television filter for the system in use in Britain (System I). The amplitude response must fit between the hatched regions.

The requirements for the centre frequency and bandwidth of this filter are such that the component is ideally suited to realisation by acoustic surface-wave techniques. The substrate size is reasonably small, yet the photolithographic definition required is within the capability of current IC technology. A conventional television i.f. filter incorporates a number of inductors that have to be individually aligned in the factory. The potential advantages of surface-wave filters – no adjustment, good reproducibility and good reliability – have obvious attractions.

The cost of a device intended for a very large consumer market is as important as its technical performance, and this fact has significantly influenced the direction of our research. The first, and perhaps the most important, decision to be made before making a filter is what to use for the substrate material. As explained earlier, the frequency response of the filter depends directly on the surface-wave velocity v, and the material must therefore have a highly reproducible value of v and one that remains sufficiently constant with temperature and time. This is particularly important for the trap frequencies, which must coincide accurately with the carrier frequencies of adjacent channels. The permissible difference in v from filter to filter is 0.25% at most, the temperature coefficient must be smaller than 120×10^{-6}/°C and ageing drift during the life of the filter (about 10 years) must be less than 0.5%.

The most commonly used material for surface-wave filters is lithium niobate, $LiNbO_3$, usually with propagation in the z-direction in a y-plane. The value of k^2 is 0.048, which is very high. However, we considered that this material was too expensive for use in a television filter. In the initial phases of our work we considered the use of piezoelectric ceramic materials, because of their low cost, but we found that the reproducibility of the surface-wave velocity v was only about 1% which was far too large to be acceptable. We therefore returned to the single-crystal materials, which are more than adequate for the reproducibility requirements.

One material that we have investigated is bismuth silicon oxide, $Bi_{12}SiO_{20}$, and most of our work has been concentrated on filters with this material as the substrate* (Ref.14). It should be a cheaper material to grow than $LiNbO_3$, since it has a lower melting point and is made from cheaper raw materials. It is not ferroelectric and so does not require polarisation. The surface-wave velocity is about half that of lithium niobate, which means that the filters are much smaller, so that more can be made from a slice of given size, thus reducing manufacturing costs. In the direction that we use (a ⟨110⟩ direction in a (100) plane), it has an acceptable value of k^2 (0.018) and a temperature coefficient of delay of 118×10^{-6}/°C.

The insertion loss of the i.f. television filter must not be too high, or the signal-to-noise ratio of the receiver will be too small. It is difficult to compensate for this by extra gain in the tuner, because of signal-handling problems. On the other hand, the insertion loss of a surface-wave filter should not be too low either, because of the triple-transit signals. If these reflected signals are not at least 40dB below the main signal, they will produce 'ghost' images in the television picture. As mentioned earlier, the triple-transit signal increases in strength as the insertion loss decreases, and its level is about twice the insertion loss plus an extra 6dB. If the triple-transit signal is at the stated level of –40dB, the insertion loss of the surface-wave filter is about 17dB. This situation would be altered if any of the schemes referred to earlier for reducing the triple-transit signal were to be used, but in the case of the television filter the associated costs would be too great. An insertion loss of 17dB is obtained from a filter on a substrate of $Bi_{12}SiO_{20}$ with a low-Q tuning inductor at one end; television receivers using such a system have been found to give a very satisfactory performance.

The details of the frequency-response requirements are not the same in the various European countries or in other parts of the world. So far we have concentrated on producing designs for System I (U.K.) and System G (the Netherlands, West Germany, etc.). The amplitude response of a filter for System I is shown in Fig.14a. This filter is a single-finger design; the uniform output transducer has 16 fingers and the input transducer 74. The substrate material is $Bi_{12}SiO_{20}$. The 'low-interaction' layout mentioned earlier is used in the input transducer, and this helps to keep the group-delay response flat to within 25ns across the passband, as shown in Fig.14b.

The other system (G) is significantly different from the British one. Here the signal is transmitted with a predistorted group-delay characteristic. This is done to compensate for the group-delay characteristics of conventional inductance-capacitance filters. This means however that the surface-wave filter must accurately reproduce this group-delay distortion. The amplitude and group-delay requirements are shown in Fig.15, together with the measured response of one of our surface-wave filters. This filter was also made on $Bi_{12}SiO_{20}$ and has a uniform output transducer with 18 fingers. In this case a 200-finger double-finger structure was used for the input transducer. As can be seen in Fig.15, both the amplitude and the group-delay characteristics lie within the tolerances. There is also good agreement between the predicted group-delay characteristic and the measured one as shown in Fig.15b. The mask used to make this filter is shown in Fig.16.

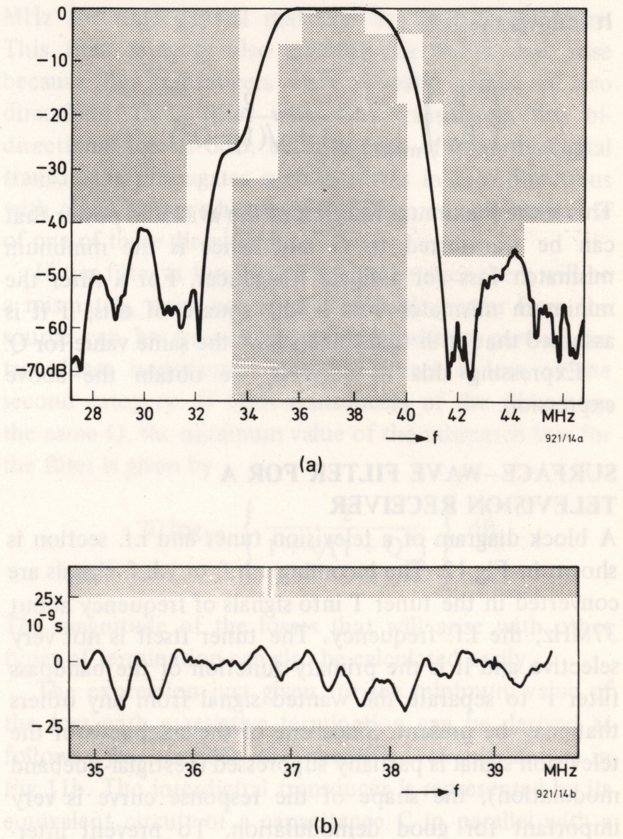

Fig.14 – (a) As Fig.13, but now including the amplitude response of one of our filters. This completely satisfies the specification. (b) The group-delay response of this filter, again with the appropriate tolerance mask.

---

*Another team at our laboratories have developed methods for making large single crystals of this material (see Ref.14).

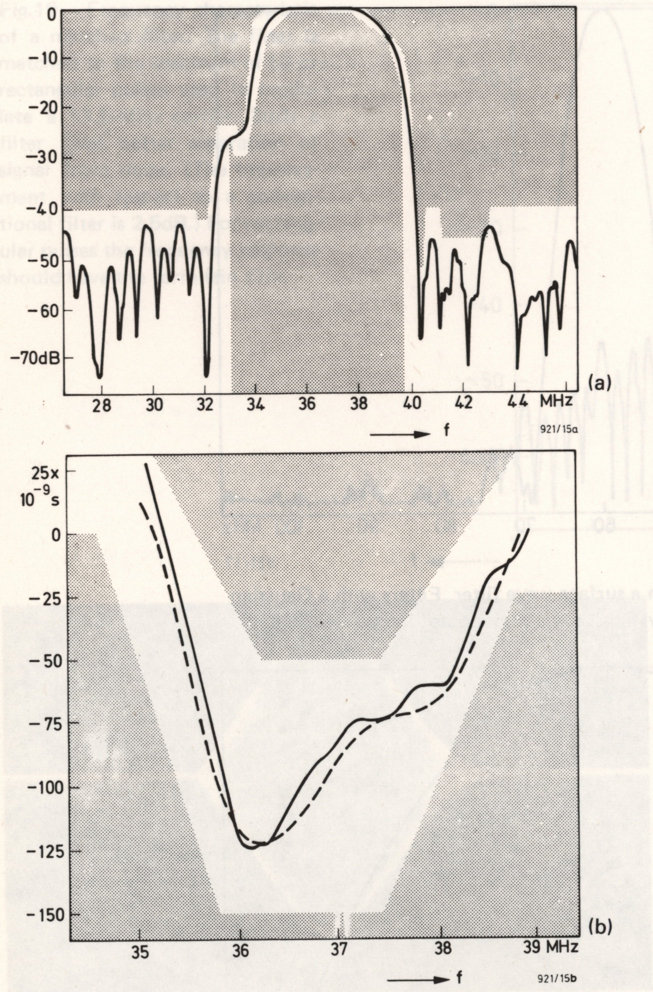

Fig.15 – (a) Tolerance mask and measured amplitude response of a television filter for system G (the Netherlands, West Germany, etc.). (b) Tolerance mask and measured group-delay response for a filter for system G. This response is designed in such a way that group-delay distortion occurring elsewhere in the system is compensated. The dashed curve is the calculated response.

OTHER FILTERS

Surface acoustic-wave filters have been designed for other applications, such as i.f. filters for radar and telecommunication. Here the cost of the filter is not such an important factor as with the television filter.

In radar, where the systems deal with pulses, the shape of the signals produced by the filter is no less important than the frequency response. This means in particular that the triple-transit echo of the surface-wave filter must be reduced to a level below –60dB. The insertion loss of a radar filter is usually designed to be between 25 and 30dB so that the triple-transit echo level is suitably low; occasionally special transducer arrangements are used that give cancellation or partial cancellation of this echo. We shall now discuss three applications of the surface-wave filter in radar and telecommunication.

Gaussian filters

One type of response that can easily be produced with a surface-wave filter is the Gaussian function. This response is of particular interest to radar engineers, as it is a shape that gives no ringing of the input pulse. Since in this application the acceptable insertion loss is fairly high, we have constructed such a filter on a $Bi_{12}SiO_{20}$ substrate with propagation of the waves in a ⟨100⟩ direction on a (110) plane. This orientation is particularly favourable for the production of surface waves without the simultaneous production of bulk waves (Ref.10). The response of such a filter with a bandwidth of 4MHz

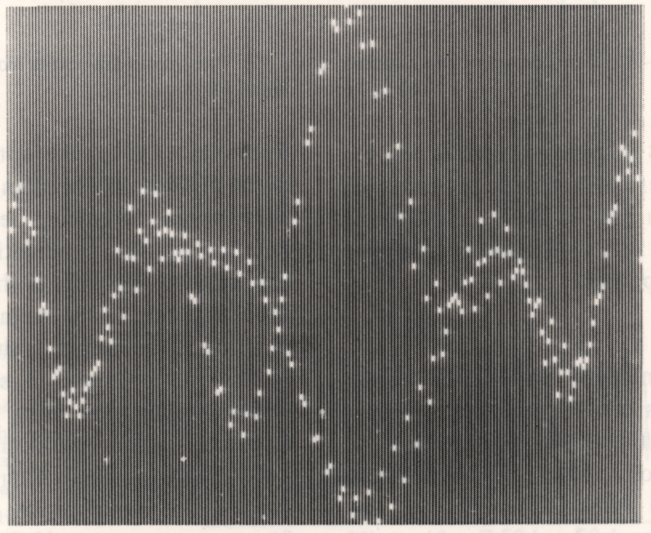

Fig.16 – A part of the mask used for making the transducers in the filter of Fig.15. This part relates to the input transducer, which has 200 fingers

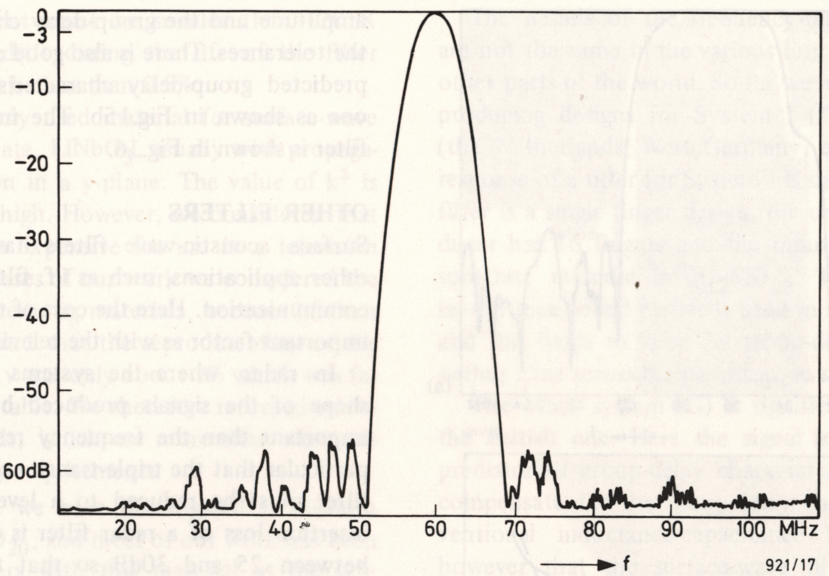

Fig.17 – Gaussian response obtained with a surface-wave filter. Filters with a Gaussian response are applied in radar systems, since they do not introduce 'ringing'

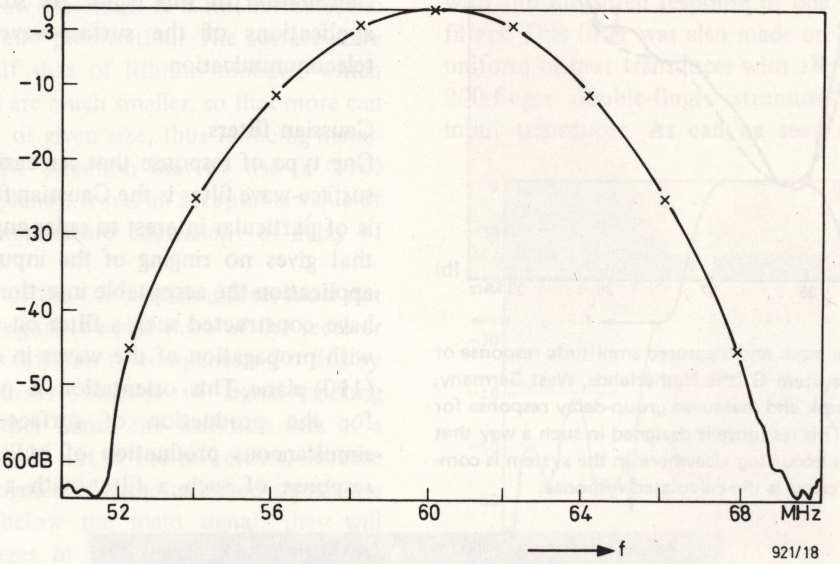

Fig.18 – The central part of the response of Fig.17. The crosses are points from the theoretical Gaussian response

(measured between the 3dB points) is shown in Fig.17; the central part of the filter characteristic is compared with the theoretical curve in Fig.18. The excellent stop-band responses are primarily due to the almost complete elimination of bulk-wave responses.

Matched filters

A class of filters that are eminently suitable for realisation as surface-wave filters is that of the matched filters. These filters are used for the optimum detection of pulses in the presence of noise. This requires that the frequency response of the filter is matched to the frequency spectrum of the received pulse. For example, the frequency spectrum of a rectangular pulse is of the form (sin x)/x; for the optimum detection of this pulse in the presence of Gaussian noise, we require a filter with an identical frequency response. For a pulse with a duration of 10μs, modulating a carrier of 13.5MHz, the (sin x)/x-like response is shown in Fig.19. The matched filter responds to the rectangular pulse with a triangular function at the output as shown in Fig.20.

The improvement in signal-to-noise ratio over the corresponding filter using only the central lobe of the response – which approximates to the usual i.f. response – is 2.5dB. Matched filters can be applied with effect only if the signal to be detected has a well defined frequency spectrum. Unfortunately, in radars that use magnetrons as the power source the spectrum is too

Fig.19 – Frequency characteristic of a matched filter. The filter is matched to the spectrum of 10-μs rectangular pulses used to modulate a 13.5-MHz carrier. Such a filter gives better separation of signal from noise. (The improvement with respect to a conventional filter is 2.5dB.) For rectangular pulses the frequency response should have the form (sin x)/x.

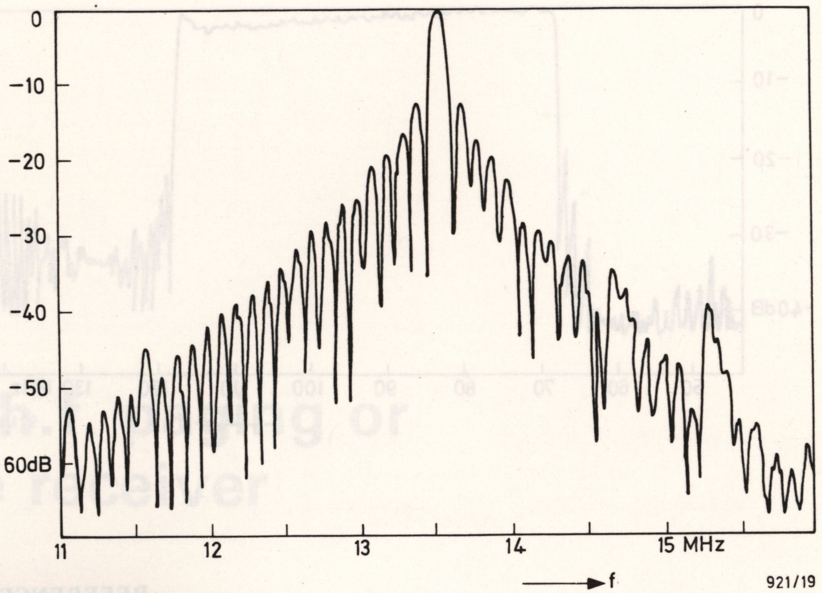

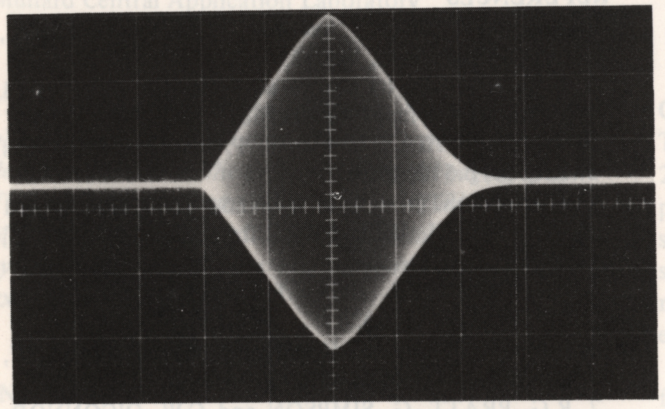

Fig.20 – Output signal from the filter of Fig.19 when a pulse of carrier frequency 13.5MHz is applied to the input to the filter.

Fig.21 – Approximation to the matched filter. The frequency response consists of the central part of the function (sin x)/x with the first two side lobes. This response was also obtained with a surface-wave filter. The improvement with respect to a conventional filter is about 1dB.

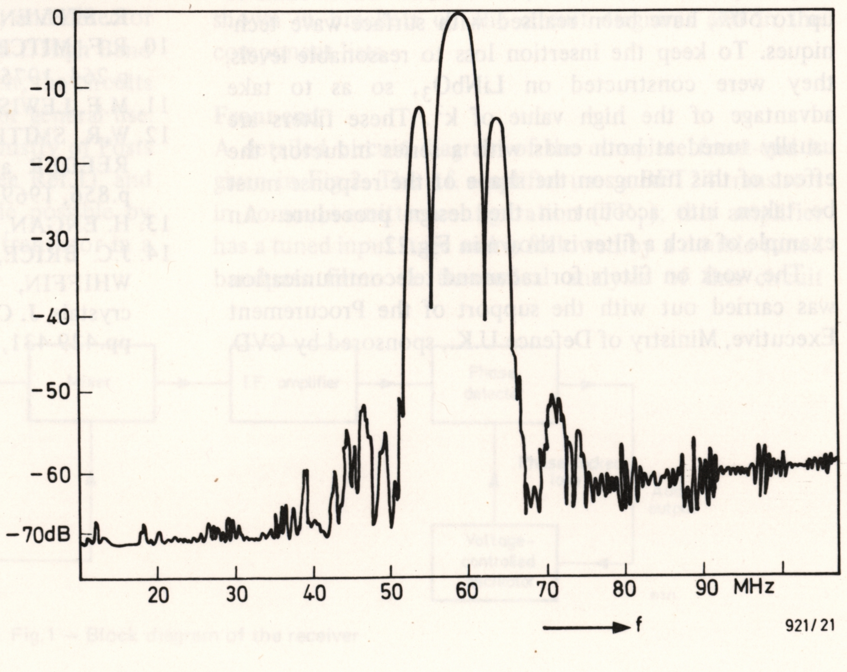

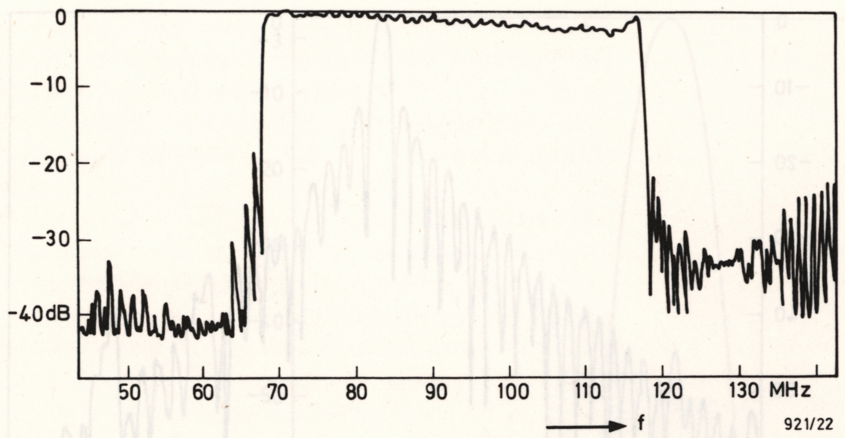

Fig.22 – Amplitude response of a wideband filter that is virtually flat from 65 to 115MHz.

ill-defined for this method to be used, and it is therefore limited to the more advanced types of radar systems.

In some situations a filter whose response is an approximation to that of a matched filter will give adequate results. As an example, Fig.21 shows a (sin x)/x response that has been limited to the central lobe and the first two side lobes. Such a response would give an improvement of about 1dB in signal-to-noise ratio, compared with that of a conventional filter. It is difficult to think of any other way of producing such a response without the use of surface waves.

Wideband filters

In telecommunication systems filters are often necessary that will have a flat frequency response over a wide frequency band. Such filters, with relative bandwidths of up to 50%, have been realised with surface-wave techniques. To keep the insertion loss to reasonable levels, they were constructed on $LiNbO_3$, so as to take advantage of the high value of k^2. These filters are usually tuned at both ends with a series inductor; the effect of this tuning on the shape of the response must be taken into account in the design procedure. An example of such a filter is shown in Fig.22.

The work on filters for radar and telecommunication was carried out with the support of the Procurement Executive, Ministry of Defence U.K., sponsored by CVD.

REFERENCES

1. R.F. MITCHELL, 'Acoustic surface-wave filters', **Philips Tech. Rev.**, Vol.32, pp.179-189, 1971.
2. K.W. MOULDING and D.W. PARKER, IEEE 1974 Ultrasonics Symp. Proc., p.168.
3. R.F. MITCHELL and D.W. PARKER, Electronics Lett.10, p.512, 1974.
4. T.W. BRISTOL, W.R. JONES, P.B. SNOW and W.R. SMITH, IEEE 1972 Ultrasonics Symp. Proc., p.343.
5. J.J. CAMPBELL and W.R. JONES, IEEE Trans. **SU-15**, p.209, 1968.
6. R.G. PRATT, G. SIMPSON and W.A. CROSSLEY, Electronics Lett.8, p.127, 1972.
7. R.G. PRATT, G. SIMPSON and C.W. O'CONNOR, Electronics Lett.10, p.369, 1974.
8. R.H. TANCRELL and R.C. WILLIAMSON, Appl. Phys. Lett.19, p.456, 1971.
9. D.E. PENNA, D.W. PARKER, F.W. SMITH and R. STEVENS, Electronics Lett.10, p.489, 1974.
10. R.F. MITCHELL and E. READ, IEEE Trans. **SU-22**, p.264, 1975.
11. M.F. LEWIS, Electronics Lett.8, p.553, 1972.
12. W.R. SMITH, H.M. GERARD, J.H. COLLINS, T.M. REEDER and H.J. SHAW, IEEE Trans. **MTT-17**, p.856, 1969.
13. H. ENGAN, IEEE Trans. **ED-16**, p.1014, 1969.
14. J.C. BRICE, T.M. BRUTON, O.F. HILL and P.A.C. WHIFFIN, 'The Czochralski growth of $Bi_{12}SiO_{20}$ crystals, J. Crystal Growth', **Philips Tech.** Vols.24/25 pp.429-431, 1974.

A low-power v.h.f. paging or pocket portable receiver

J.A. GARTERS
Mullard Central Application Laboratory

This article describes the front-end, i.f. amplifier, and phase-locked loop detector sections of a portable receiver designed for use in the proposed national paging system. The receiver conforms with the specifications of the Ministry of Posts and Telecommunications for this system, and has a very low current consumption to extend battery life.

INTRODUCTION

The proposal of a nationwide paging system, with an allocated band of 153.1 to 153.275MHz, has led to a need for portable paging receivers with the high packing density and low current consumption required to take full advantage of the system. The r.f., i.f., and detector stages of such a receiver operating in the v.h.f. High Band are described, and performance details given; the circuits may also be used in a portable receiver for general use. This paging receiver conforms with the Ministry of Posts and Telecommunications specifications (see Ref.1), and has a very low current consumption made possible by the use of the BFT24 low-voltage u.h.f. transistor in a number of positions.

CIRCUIT DESCRIPTION

The receiver is a single-conversion superhet with an i.f. of 23.455MHz and a phase-locked loop detector; the complete system is shown in block diagram form in Fig.1. The single conversion superhet configuration considerably simplifies the overall design and eases the image rejection requirements, which are always a problem in portable equipment where the r.f. coils are necessarily small.

The circuit can be considered in three parts: the front-end (including oscillator, mixer, and r.f. amplifier circuits); the i.f. amplifier; and the detector. Each part is described in the following sections. Any component type number mentioned refers to devices in standard encapsulations; alternative types for microminiature versions are shown in brackets on the circuit diagrams and in the component lists.

Front-end

A detailed circuit diagram of the complete front-end is given in Fig.2. The r.f. amplifier uses a BFT24 transistor in common-emitter configuration (TR_1); this amplifier has a tuned input stage and is followed by a double-tuned bandpass filter. A theoretical analysis of this circuit

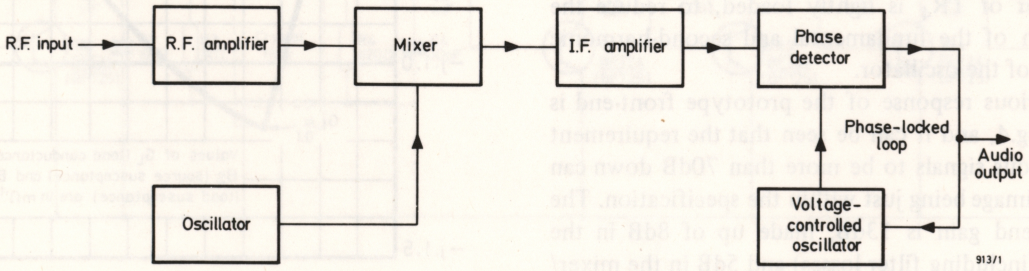

Fig.1 — Block diagram of the receiver

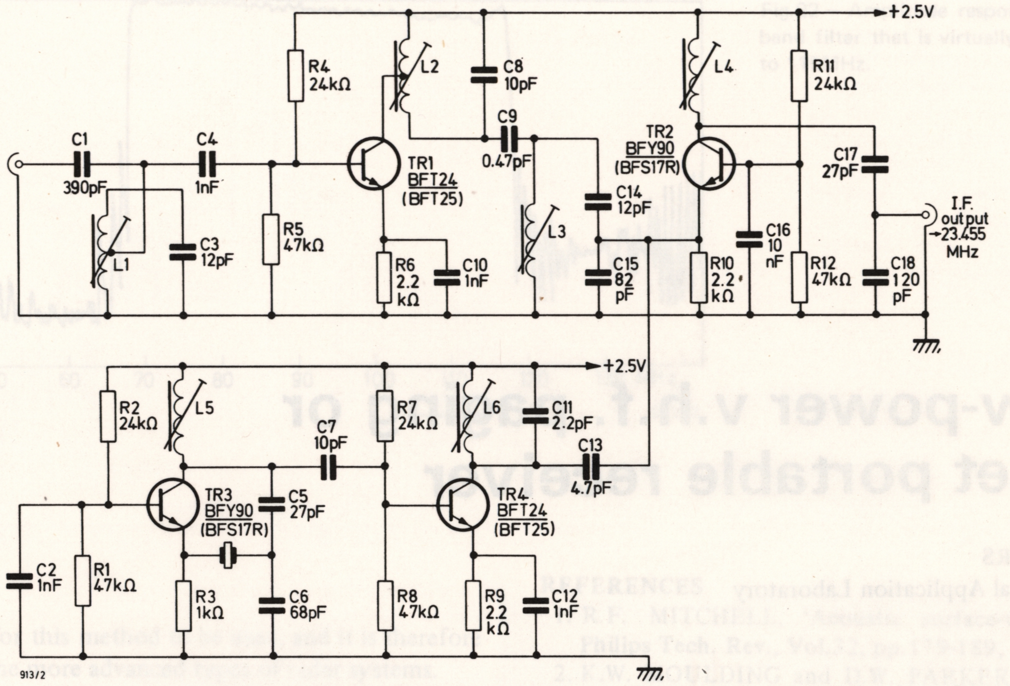
+2.5V
R.F. input →162 MHz
C1 390pF
L1
C4 1nF
C3 12pF
R4 24kΩ
R5 4.7kΩ
L2
C8 10pF
TR1 BFT24 (BFT25)
R6 2.2 kΩ
C10 1nF
C9 0.47pF
L3
C14 12pF
C15 82 pF
TR2 BFY90 (BFS17R)
L4
R11 24kΩ
R10 2.2 kΩ
C16 10 nF
R12 4.7kΩ
C17 27pF
C18 120 pF
I.F. output →23.455 MHz
R2 24kΩ
L5
C2 1nF
R1 4.7kΩ
TR3 BFY90 (BFS17R)
C5 27pF
R3 1kΩ
C6 68pF
C7 10pF
R7 24kΩ
L6
C11 2.2pF
C13 4.7pF
TR4 BFT24 (BFT25)
R8 4.7kΩ
R9 2.2 kΩ
C12 1nF
913/2

Fig.2 — Front-end circuit

indicates that a minimum Q-factor of 140 is required for the coils used in the tuned circuits if the 70dB image rejection requirements specified in Ref.1 are to be met. Work done to date suggests that for v.h.f. operation it is not possible to print coils with a Q-factor much above 50; it follows that the r.f. tuning coils must be external to the module if the receiver is constructed using hybrid thick-film technology.

The loop gain of the amplifier under various tuning conditions and with various collector loads is shown in Fig.3. A source resistance (R_s) of 300Ω was used for optimum noise performance, but it can be seen that the amplifier is still stable with the input open-circuited, because the loading of the coil gives a source resistance of 1kΩ with the aerial disconnected.

The mixer circuit uses a BFY90 transistor in common-base configuration, this transistor (TR_2) being found to give slightly better signal handling than the BFT24 at the power levels used, probably because of the larger chip. The local oscillator is a 62MHz crystal oscillator (TR_3) followed by a frequency trebler (TR_4), and injects about 100mV at the emitter of the mixer. The tuned circuit at the collector of TR_4 is lightly loaded, to reduce the feed-through of the fundamental and second-harmonic frequencies of the oscillator.

The spurious response of the prototype front-end is shown in Fig.4, and it can be seen that the requirement for all spurious signals to be more than 70dB down can be met, the image being just within the specification. The total front-end gain is 13dB, made up of 8dB in the transducer (including filter losses) and 5dB in the mixer/oscillator section.

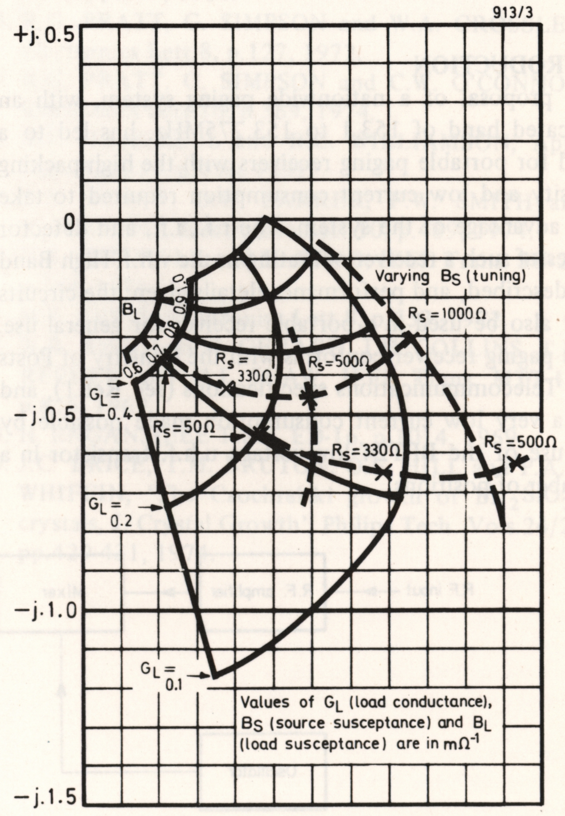

Fig.3 — Loop gain of r.f. amplifier

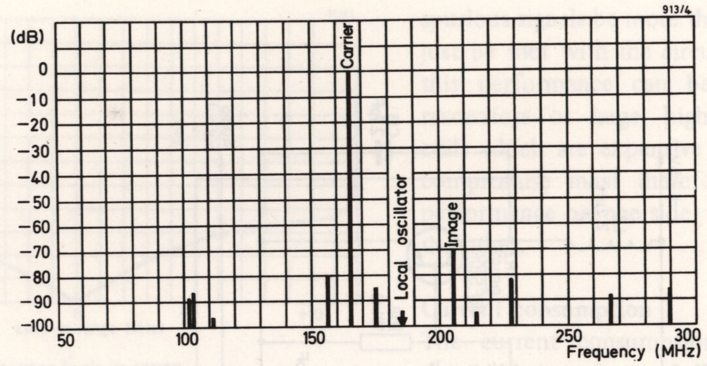

Fig.4 — Spurious response of complete front-end

I.F. amplifier

A detailed circuit diagram of the i.f. amplifier stage of the receiver is given in Fig.5. This section uses five BFT24 transistors (TR_1 to TR_5) in a wideband amplifier, with a 23.455MHz crystal filter inserted between the first two stages to give i.f. selectivity.

The results of a computer-aided a.c. analysis of the wideband amplifier, using a hybrid-π model, indicate a gain spread of 70 to 75dB, assuming that the gain of the BFT24 varies from 30 to 100.

The current consumption for each stage may be calculated from:

$$I_C \simeq \frac{h_{FE}(V_{CC} - V_{BE})}{R_F + h_{FE} R_L}, \qquad \ldots(1)$$

where I_C is the collector current of a transistor stage and V_{BE} its base-emitter voltage, h_{FE} is the gain of the transistor, V_{CC} is the supply voltage (2.5V), R_F is the feedback resistance, and R_L is the collector load resistance. If V_{BE} is taken to be −0.7V for the BFT24, and the component values from Fig.5 inserted, Eq.1 gives a spread of values for the current from 201 to 214μA where the h_{FE} spread is 30 to 100. The current consumption of the entire amplifier is thus about 1mA at 2.5V.

The noise figure of the amplifier is 5.5dB when the source impedance is 300Ω, and as the front-end gain is 13dB the total noise figure of the receiver should depend only slightly on the i.f. noise figure.

Phase-locked loop detector

The detector section is a phase-locked loop type, and includes some novel features; the circuit diagram of this section is shown in Fig.6. The i.f. input signal is phase-split in TR_1, and the two signals fed to the inputs (pins 2 and 3) of the TCA520B operational amplifier (IC_1). The signal from the voltage-controlled oscillator (VCO) is fed in parallel to these inputs, and the IC operates as a phase detector; it will be noted that in this configuration pins 1 and 8 of the IC are not connected. The output is applied via a loop filter to a variable-capacitance diode (D_1), which controls the frequency of the crystal oscillator TR_2. The crystal is a third-harmonic series-resonant type used at its fundamental frequency of 7.818MHz to give the best pulling range, which is an important factor in the successful operation of a phase-locked loop for narrowband f.m. detection. The output signal from TR_2 is then frequency trebled in TR_3, giving a VCO output at 23.455MHz. The gain of the operational amplifier is set at 30dB, and the maximum variation of the output is ±1.25V which shifts the crystal oscillator frequency by ±4kHz in the circuit shown. After frequency trebling,

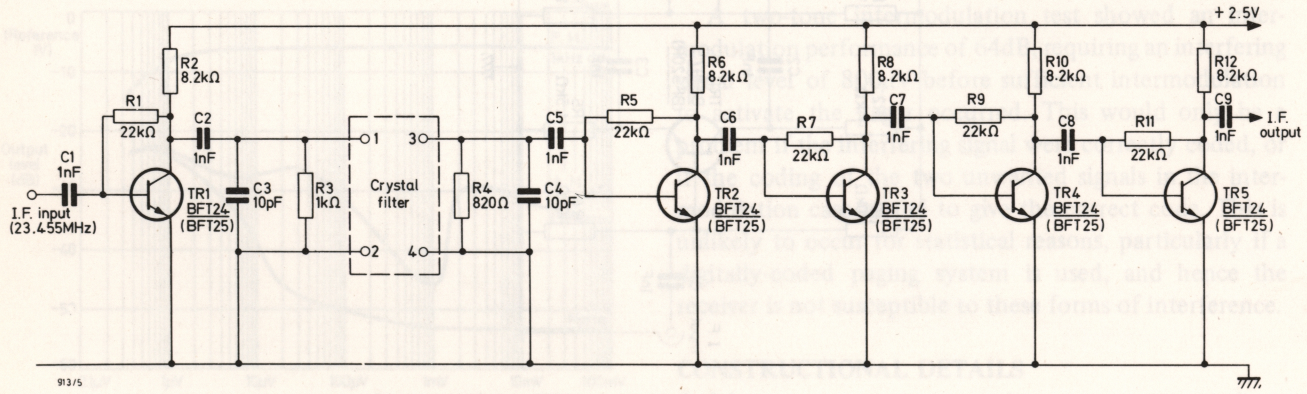
+2.5V
R2 8.2kΩ
R1 22kΩ
C1 1nF
I.F. input (23.455MHz)
C2 1nF
TR1 BFT24 (BFT25)
C3 10pF
R3 1kΩ
Crystal filter
1
2
3
4
R4 820Ω
C4 10pF
C5 1nF
R5 22kΩ
R6 8.2kΩ
C6 1nF
R7 22kΩ
TR2 BFT24 (BFT25)
R8 8.2kΩ
C7 1nF
R9 22kΩ
TR3 BFT24 (BFT25)
R10 8.2kΩ
C8 1nF
R11 22kΩ
TR4 BFT24 (BFT25)
R12 8.2kΩ
C9 1nF
I.F. output
TR5 BFT24 (BFT25)
913/5

Fig.5 — I.F. amplifier circuit

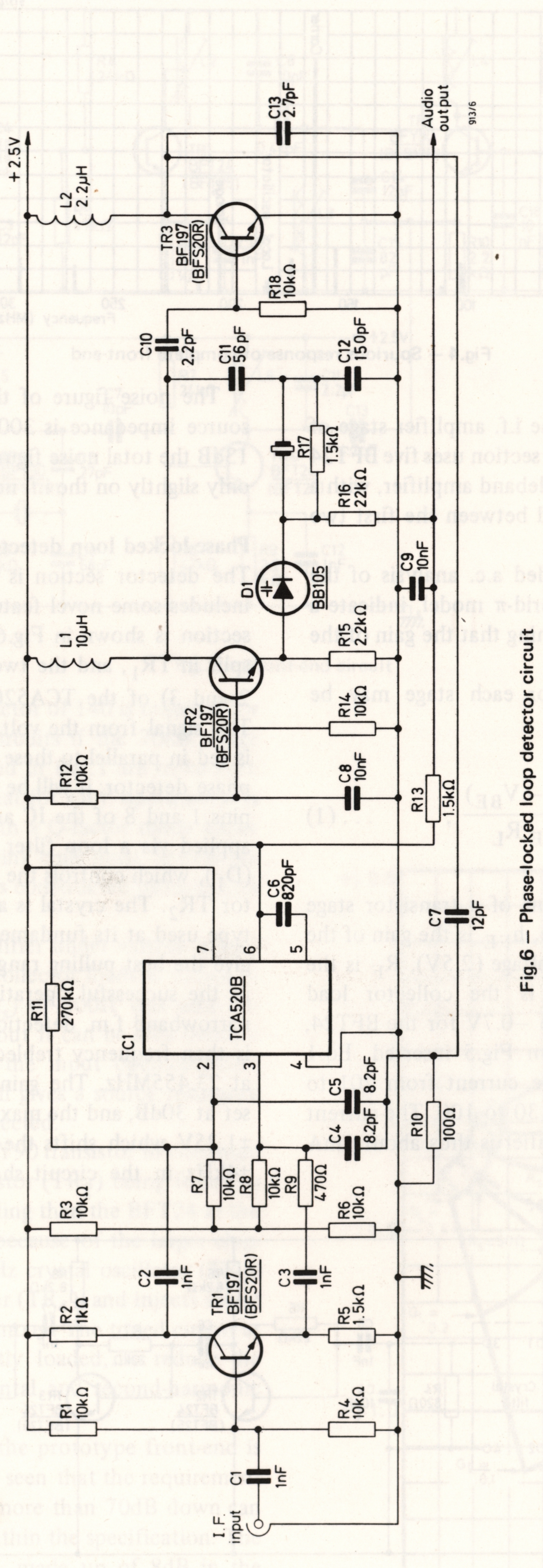

Fig.6 – Phase-locked loop detector circuit

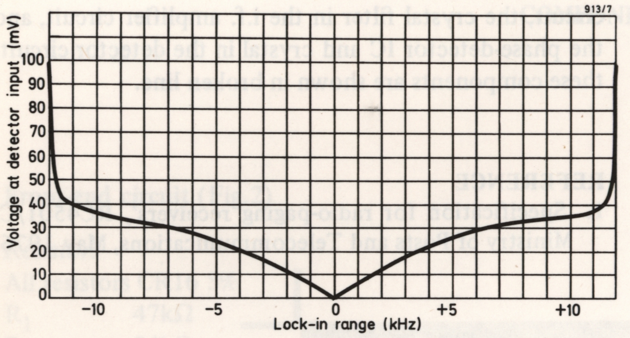

Fig.7 – Detector lock-in range

therefore, the VCO output can be deviated by ±12kHz, as shown in Fig.7 which shows the lock-in range. The a.f. output level is 1.2V pk-pk for a 5kHz deviation and a 1kHz modulation frequency.

RECEIVER PERFORMANCE

Sensitivity

Curves showing the sensitivity and a.m. rejection of the complete receiver are shown in Fig.8. The level at which the decoder will activate a paging signal depends to some extent on the design of the decoder to be used, but a signal-to-noise ratio of 10dB would be more than adequate, and hence the pager may be expected to operate at an input voltage of 0.3µV. However, this result is slightly misleading, as at the input of the phase detector the level of the i.f. signal with a 0.3µV r.f. input signal is about 20dB below the limiting level. The lock-in range is thus reduced to about ±1kHz (from Fig.7) and the peaks of the a.f. output become distorted. For a paging receiver this is not a very important drawback, but for a portable receiver the i.f. gain should be increased to reduce the input level necessary for limiting.

Selectivity

The adjacent channel selectivity is defined by the crystal filter in the i.f. amplifier, and is greater than 80dB for a channel spacing of 25kHz. The requirement that all spurious signals be more than 70dB down (see Ref.1) can just be met with the circuit shown; an improvement in this performance can be obtained by using helical resonators or large, high-Q-factor mechanically-stable coils which are expensive and occupy a lot of space. A compromise must therefore be found between good performance on one side, and large size and expense on the other.

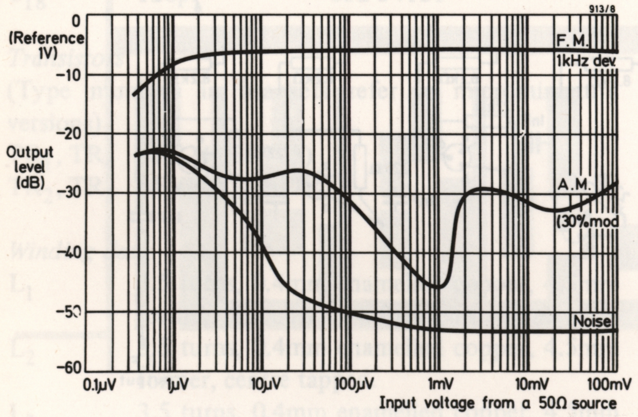

Fig.8 – Sensitivity and a.m. rejection of the complete receiver

Current consumption

The current consumption of the receiver shown is detailed below, from a 2.5V supply.

Front-end	1.4mA
I.F. amplifier	1.0mA
Detector	3.8mA
Total	6.2mA

The power consumption is therefore 15.5mW. It is possible that a lower current consumption in the detector section may be achieved by modifying the VCO circuit, with a consequent reduction in overall power consumption.

If a 500mA/hour battery with a 10:1 duty cycle battery-economy circuit is used, and the receiver operated for 12 hours a day, a battery life of 14 weeks is possible.

Blocking

The receiver described blocks at an input level of 3mV for a 3dB reduction in signal-to-noise ratio. This indicates that the blocking specification given in Ref.1, that there be a 70dB difference between the just-operate input signal level and the interference signal level, can be met.

Crossmodulation and intermodulation

Performance requirements for these types of interference are not included in the specifications given in Ref.1, probably because the interfering signals, although producing in-band spurious responses, will not be correctly coded and will not therefore activate the pager.

A two-tone intermodulation test showed an intermodulation performance of 64dB, requiring an interfering signal level of 800µV before sufficient intermodulation to activate the pager occurred. This would only be a problem if the interfering signal were correctly coded, or if the coding of the two unwanted signals in the intermodulation case mixed to give the correct code. This is unlikely to occur for statistical reasons, particularly if a digitally-coded paging system is used, and hence the receiver is not susceptible to these forms of interference.

CONSTRUCTIONAL DETAILS

A laboratory prototype receiver was constructed on three single-sided printed-wiring boards, to simulate the

Phase-locked loop detector circuit (Fig.6)

Resistors

All resistors CR16 5%

R_1	10kΩ
R_2	1kΩ
R_3	10kΩ
R_4	10kΩ
R_5	1.5kΩ
R_6	10kΩ
R_7	10kΩ
R_8	10kΩ
R_9	470Ω
R_{10}	100Ω
R_{11}	270kΩ
R_{12}	10kΩ
R_{13}	1.5kΩ
R_{14}	10kΩ
R_{15}	2.2kΩ
R_{16}	22kΩ
R_{17}	1.5kΩ
R_{18}	10kΩ

Transistors

(Type number in brackets refers to microminiature version)

TR_1, TR_2, TR_3	BF197 (BFS20R)

Capacitors

C_1	1nF	629 06102
C_2	1nF	629 06102
C_3	1nF	629 06102
C_4	8.2pF	632 09828
C_5	8.2pF	632 09828
C_6	820pF	630 02821
C_7	12pF	632 10129
C_8	10nF	629 06103
C_9	10nF	629 06103
C_{10}	2.2pF	632 09228
C_{11}	56pF	632 34569
C_{12}	150pF	632 34151
C_{13}	2.7pF	632 09278

Inductors

Painton sub-miniature chokes

L_1	10μH	58/10/00011
L_2	2.2μH	58/10/0007

Diode

D_1	BB105

Integrated circuit

IC_1	TCA520B